Misr University for Science and Technology

College of Engineering

Department of Mechatronics Engineering

Fall 2023-2024

Earthquake shaking table

By: GROUP (8)

Name	**ID**
Ahmed Mohamed Ibrahim	80860
Arsany Naem	80718
Alhassan Abdelhamid	80854
Yunes Robian	75541

Supervised By:

Dr. Bahaa Eldin Mohamed Naser

Prof. Dr. Mohamed Hamdy

Prof. Mohamed Ibrahim

Assoc. Prof. Dr. Tahany William

Dr. Ahmed Sabry

DEDICATION

To all our parents who taught us since childhood and watched us nights. We would like to dedicate this project to you, where you can see with your own eyes the merit of this hard work that you worked for us, which made our character and led us to become real engineers

Signed: ______________________

Date:

Signed (repeat for all students) :

Ahmed Mohamed Ibrahim

Arsany Naem

Alhassan Abdelhamid

Yunes Robian

Acknowledgment

First, we would like to express our deepest gratitude and appreciation to our parents for their unwavering love, support, and guidance throughout our life. Their constant encouragement and motivation have been a driving force behind our achievements and successes.

And also, we would like to express our heartfelt appreciation to our advisors, for their unwavering support of our study and research, as well as their patience, encouragement, inspiration, and vast knowledge. Their advice was invaluable throughout the research and writing of this thesis. We could not have asked for better advisors and mentors for our project. Finally, we would like to show our special thanks to the department's head, Prof. Dr. Bahaa Eldin.

Abstract

This unidirectional shake table test delves into the seismic performance of a specimen type under simulated earthquake motions. Secured on the platform, the specimen faces a meticulously curated sequence of ground motions mimicking diverse earthquake scenarios. Throughout the tremors, its acceleration, displacement, and strain responses are meticulously monitored and captured. A thorough data analysis then dissects its dynamic properties, earthquake-resistant capacity, and overall resilience. This unveils valuable insights into its seismic behavior, validates numerical models for enhanced accuracy, and ultimately informs the development of robust earthquake-resistant design strategies.

Table Of Contents

List of Tables

List of figures

قسم هندسة الميكاترونيات | قسم هندسة التشييد

السيد/ رئيس قسم هندسة الميكاترونيات

السيد / رئيس قسم هندسة التشييد

تحية طيبة

الموضوع/ تعاون في تنفيذ مشروع تخرج 2023-2024 Uni-axial Shaking Table

بالاشارة إلى الموضوع أعلاه , حيث يقوموا طلاب هندسة الميكاترونيات مجموعة(8) بتنفيذ المشروع بالموصفات التالية:

Specifications of System Design	Value of Specification
Shaking direction	Uni-axial horizontal motion
Dimension of shake table	60× 40cm
Dimension of shake table	10cm
Maximum load weight	10kg
Amplitude range	1-80 mm
Control system	dedicated software running under a PC
Engine	Stepper motor

و عليه فإن الزملاء طلاب هندسة التشيد يقوموا بتنفيذ نماذج هياكل الاختبار . ومن ثم نقوم معا(طلاب هندسة الميكاترونيات و طلاب هندسة التشيد) بإجراء الاختبارات على المشروع ومقرنتها بالوقع خلال شهر ابريل 2024

ولكم جزيل الشكر والتقدير

رئيس قسم هندسة الميكاترونيات

رئيس قسم هندسة التشيد

Ahmed Sayed

Chapter 1
Introduction

1.1 Introduction

Earthquakes

The Earth, often perceived as a stable platform, occasionally unleashes its raw power through earthquakes – sudden and violent shaking of the ground that can leave a trail of destruction in its wake. These events, a stark reminder of Earth's dynamic nature, have captivated and terrified humanity for centuries.

The Trembling Earth:

Sudden Ground Motion: Earthquakes are not mere tremors, but violent shaking of the Earth's surface caused by the movement of tectonic plates, Earth's colossal puzzle pieces constantly shifting beneath our feet.

Widespread Devastation: The consequences of earthquakes can be far-reaching, causing widespread damage to infrastructure, triggering landslides and tsunamis, and even altering landscapes.

Magnitude Matters: The severity of earthquakes is measured on the Richter magnitude scale, a logarithmic scale ranging from 1 (barely perceptible) to 10 (capable of reshaping entire regions).

Plate Tectonics: The Earth's outermost layer, the lithosphere, is not a monolithic shell but a fragmented mosaic of massive, rigid plates constantly in motion due to the convection currents within the Earth's mantle.

Friction and Release: These plates grind against each other, slide past, or occasionally collide, building up immense frictional forces. When this tension reaches a critical point, it releases energy in the form of seismic waves, causing the ground to shake.

Seismic Waves: The energy released during an earthquake travel through the Earth's interior as seismic waves, causing the ground to vibrate sometimes for hundreds of miles around the epicenter, the point on the surface directly above the rupture.

The crust can move vertically or horizontally because of fault movements.

If the crust moves vertically, scientists say it has been uplifted. Vertical movements create a sharp edge called a fault scarp. If the crust moves horizontally we say it has been offset or displaced .

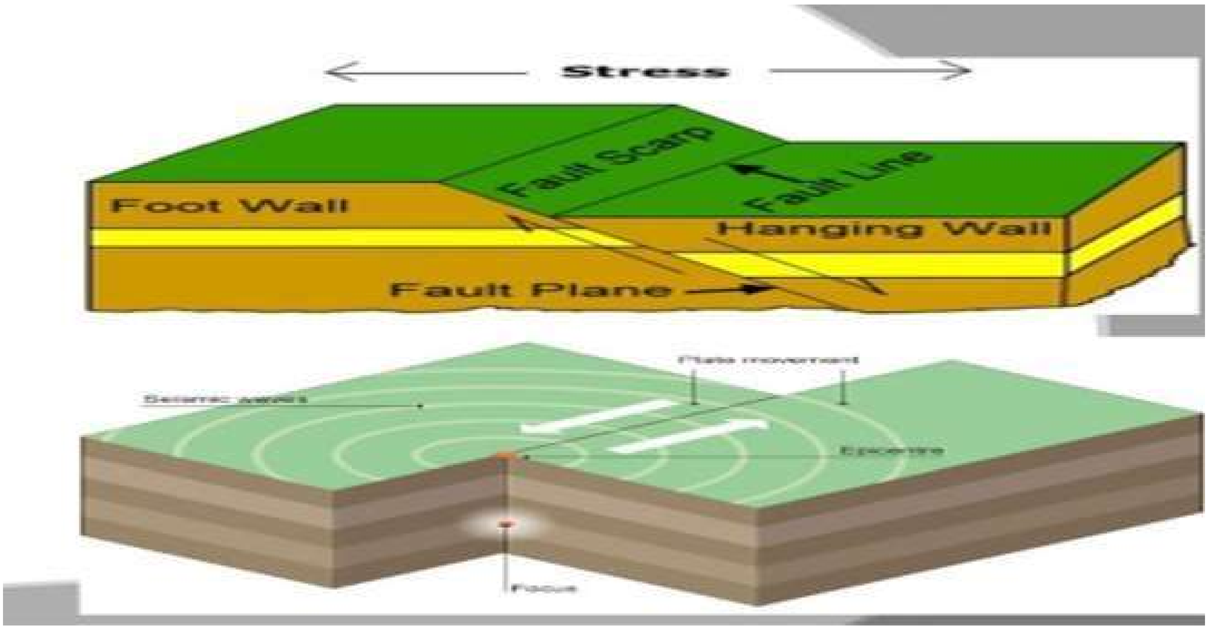

fig 1.1 s-wave, p-wave direction

to the direction of particle motion. Vertically and horizontally polarized S-waves are known as SV-wave and SH-wave, respectively. They are sometimes called secondary waves because they travel more slowly than P-waves in the same material. S-waves do not change the instantaneous.

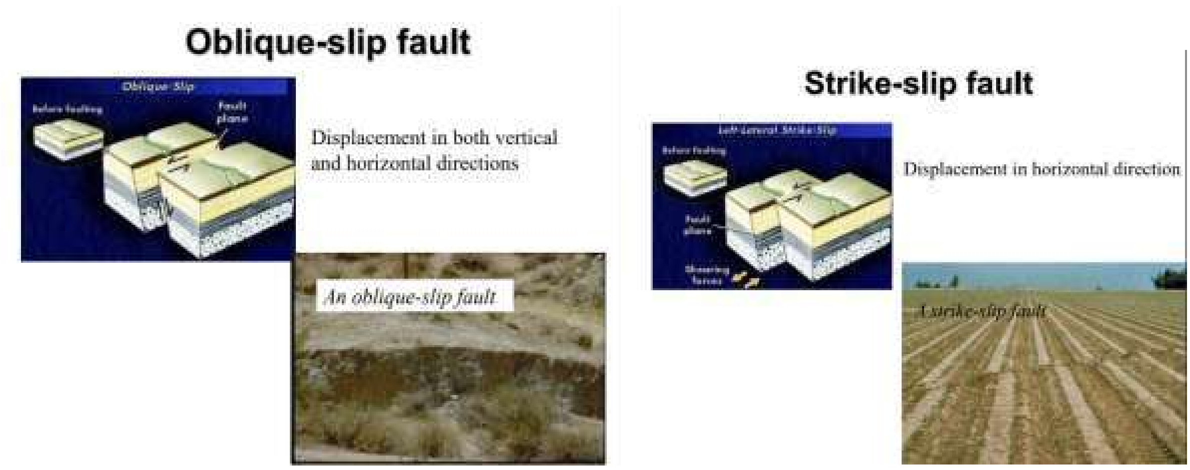

Fig1.2 type fault

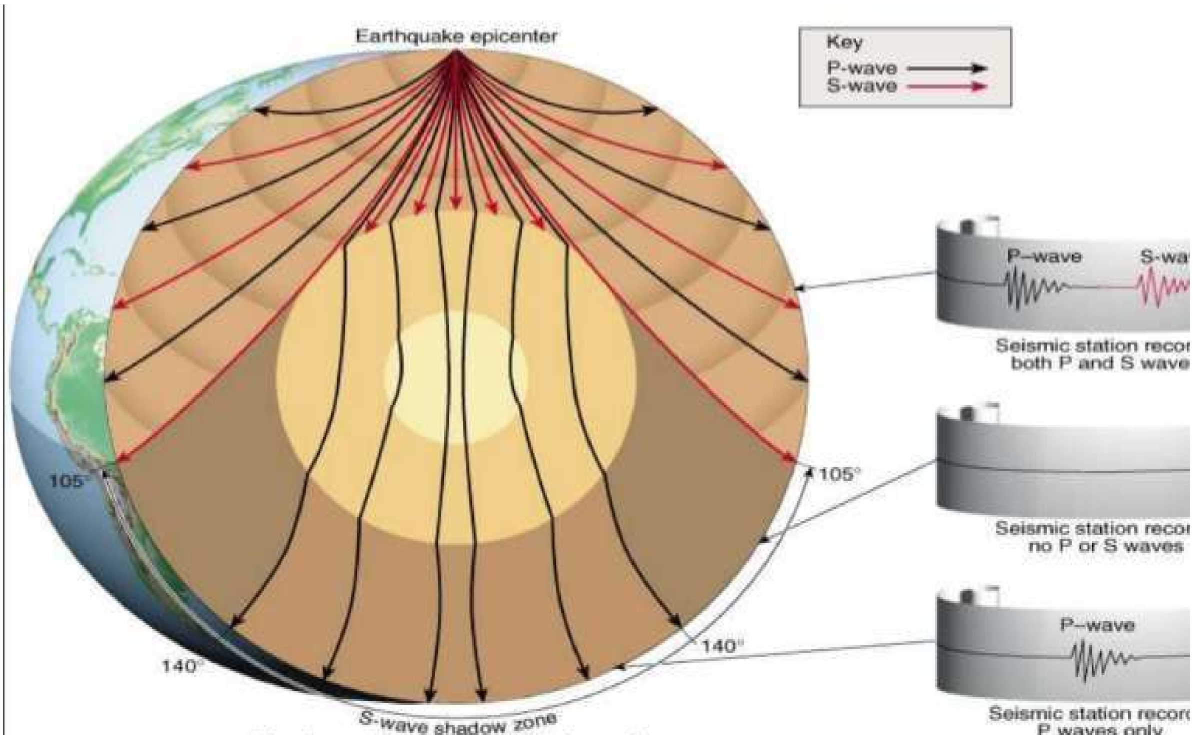

Shadow Zone - no earthquake waves

1.2 Shake table introduction.

Comparing theoretical results to the dynamic behavior of structures using scaled structure models is a preferred research method in civil engineering. To facilitate this, a shake table equipped with Arduino microcontroller boards, has been developed for earthquake simulations. The horizontal components of the acceleration records obtained from past earthquakes are scaled and transferred to the shake table using software programs developed with an Arduino board. The seismic ground motion along the horizontal axis is transferred to the shake table via a linear actuator system built with a ball screw assembly, linear bearings, and a DC motor. In the advanced uniaxial vibration mechanical system of the shake table table, precision linear ball bearings and a slide assembly are used to reduce friction on the slides on which the 16mm crow balls move. The base of the table measures 62mm by 40mm, while the top measures 35mm by 35mm. The slats are fixed with suitable supports, and in the prototype stage, the top and bottom panels are manufactured from 18 mm thick MDF board using CNC machining.

The linear actuator assembly used for driving the single-phase displacement-controlled vibration table is constructed from a two-phase DC motor. Arduino transmits control signals. The presented SARSAR shaking table can perform simple single and damped harmonic motions of different amplitudes and frequencies and simulate seismic ground motion using developed Arduino software. The shaking table is calibrated with different amplitude and frequency responses for simple harmonic motion, with channel measurements at 200 Hz for six-channel measurements, which is sufficient to observe the dynamic behavior of the shake table. The Arduino code for the data acquisition part of the control unit is provided in the online resource.

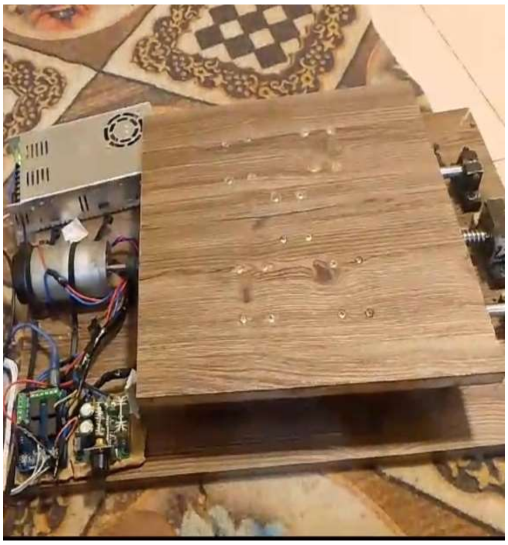

1.3 data acquisition using PLX DAQ v2.

PLX DAQ v2 is a program used to establish an easy communication.

between Microsoft Excel on a Windows Computer and any device that supports serial port protocol. It was intentionally written to allow communication. between Arduino and Excel.
you can, for example, measure temperature data with your Arduino, send the results to Excel every 10 seconds, print the data on a sheet and draw a graph with all information.

All communication will be done by **Serial.println** commands just like the commands you use to send from Arduino to monitor in your Arduino IDE Serial Monitor.

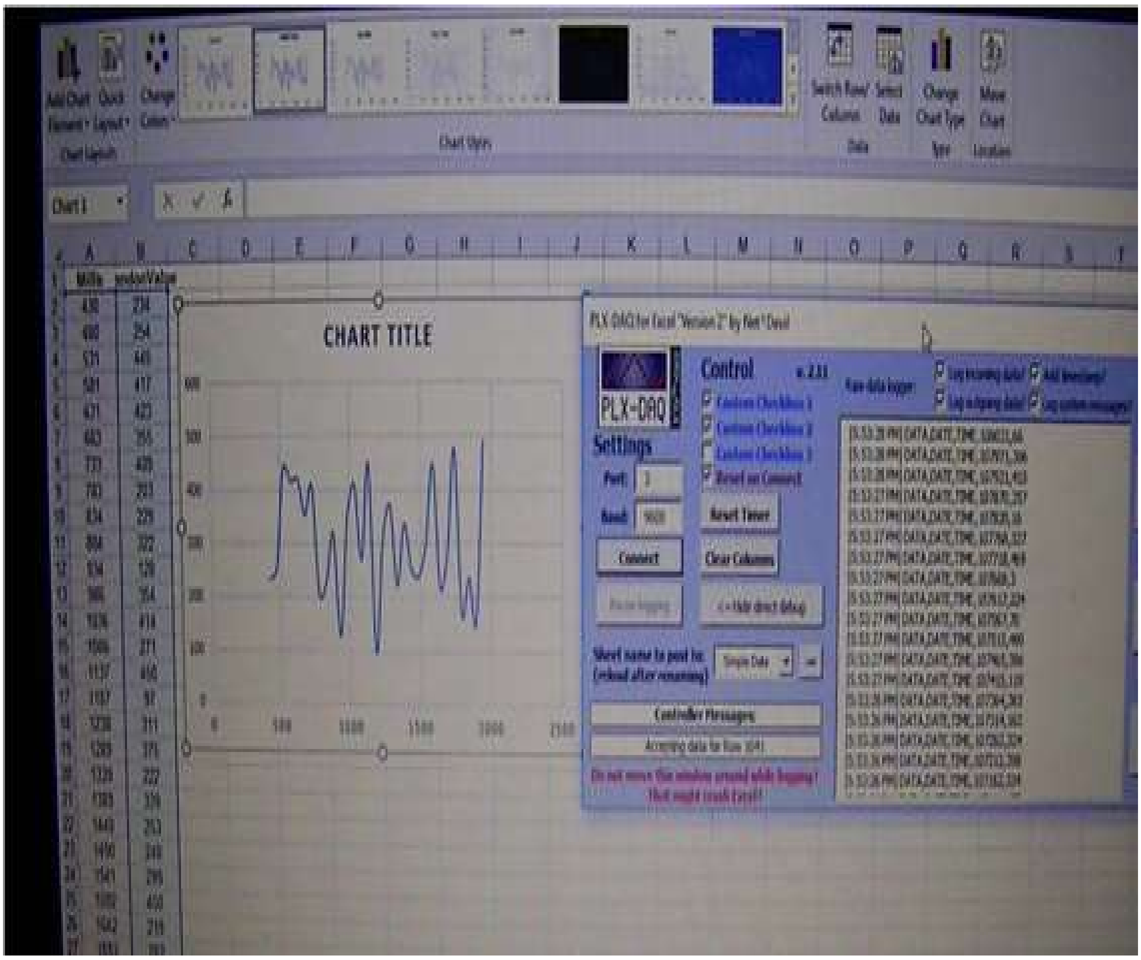

Fig1.3 data acquisition

1.3 Liquefaction Using Shake Table Test

One of the major causes of destruction during an earthquake is the failure of the ground structure. The ground may fail due to fissures, abnormal or unequal movement or loss of strength. The loss of strength may take place in sandy soils due to increase in pore pressure. This phenomenon is termed as liquefaction. The increase in pore pressure is due to shaking of ground.
Naturally occurring earthquakes are a major source of vibration of ground soil. The waves produced during an earthquake are random in nature which are responsible for liquefaction. Thus earthquake induced liquefaction leads to detrimental effects to a larger extent and thus is to be assessed. The hazards caused due to liquefaction could be of various types such as flow failure, lateral spreads, development of fissure and cracks, loss of strength, increased lateral pressure on retaining walls etc.

1.3.1 **Test Procedure**

The specific values of frequency and amplitude are set on the shake table apparatus. Then the box model 300mm x 200mm x 150mm is fixed to the base plate of the equipment. for the convenience of specimen preparation. The calculated amount of sand and water are weighted accurately. and the soil model filled in layers. The care is taken to achieve required density, corresponding to a particular relative density.

Fig1.3.1 the box model test

Amplitude is then set on the instrument and frequency is adjusted digitally on the display shows Thereafter, the equipment is switched on which starts shaking the soil in the model at the required acceleration. The data of acceleration versus time is recorded through data acquisition system.

Fig1.3.2 shaking the soil in the model

1.3.2 **Results**

Results showed that sand soils have a liquefaction potential. In addition, acceleration and relative density has a great effect on the dynamic behavior of

the soils

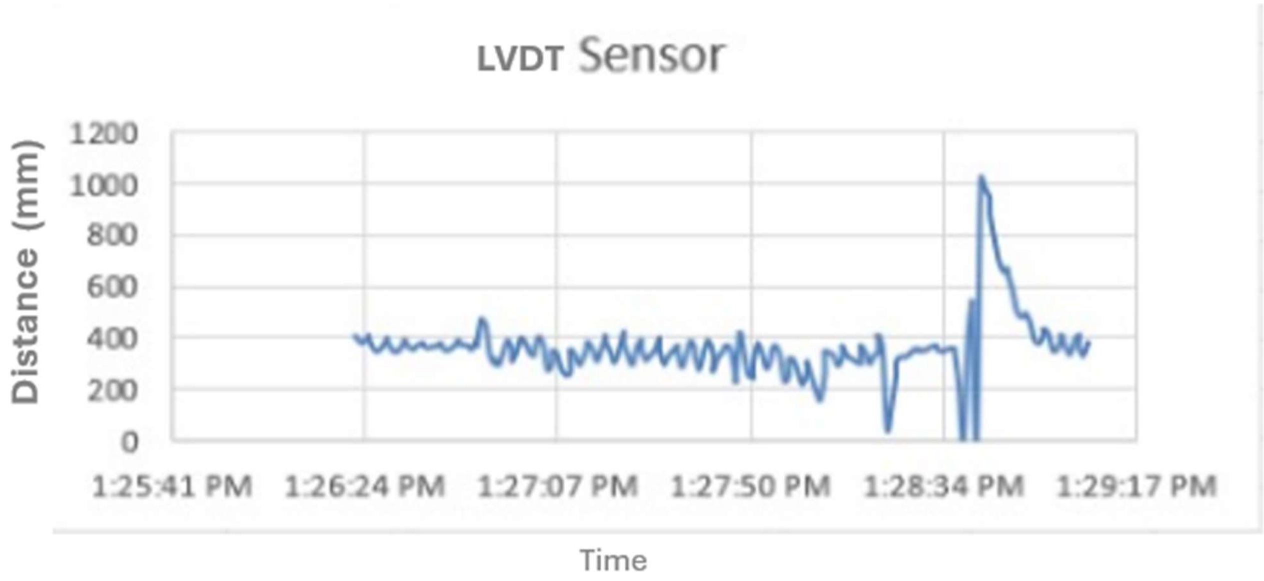

Fig1.3.3 LVDT senor Results

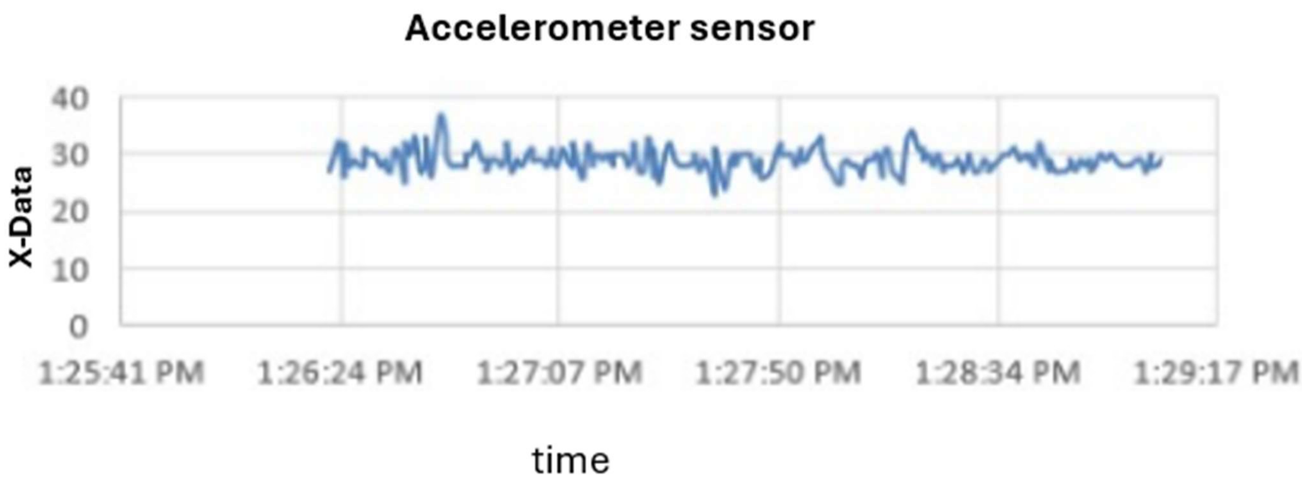

Fig1.3.4 **Accelerometer** senor Results

Literature Review
Chapter 2

2.1 Market 3D Machine alternatives

BACKGROUND: THE NEED FOR A LARGE-SCALE EARTHQUAKE TEST FACILITY

In 1995, the Hyogoken-Nanbu (Kobe) earthquake caused devastating damage to numerous buildings and the infrastructure in the Kobe area. However, this was not the first large Japanese earthquake. Along the Pacific Coast of Japan there is an ocean ridge called the Nankai Trough. The trough consists of three regions (Tokai, To Nankai, and Nankai), and slips and ruptures have occurred periodically in these regions. One or two of the regions ruptured in some cases while all three regions ruptured simultaneously in other cases. It is well known from historical records that these slips and ruptures in the Nankai Trough have caused several extremely large earthquakes over the past 500 years. Also, the interval between these super earthquakes is between 100 and 150 years. Even though no scientific prediction data exist, calculating from the pattern of previous large earthquakes, it is likely that Japan will be hit by very large earthquakes in the middle of the twenty-first century [1].

The Council of National Disaster Mitigation, chaired by the Prime Minister of Japan, reported in 2005 that, when the three regions of the Nankai Trough rupture at the same time, about 1 million buildings will collapse, about 25 000 people may lose their lives, and the economic loss will be 1 trillion US dollars. From these data, the earthquake danger is the most critical national problem in Japan. The 1995 Kobe earthquake and other recent large earthquakes have made the following two facts clear [2].

1. Throughout Japan, many old buildings and infrastructures exist whose seismic capacity is insufficient. To prepare for future large earthquakes, it is crucial to evaluate their seismic capacities accurately and strengthen them according to the evaluation results using appropriate retrofit technologies.

Since severe earthquake ground motions that would cause structural collapse to occur very rarely, it is difficult to monitor or measure the real behaviour of structures subjected to such events. Furthermore, building structures are massive and mostly beyond the capacity of existing laboratory test facilities, while miniature models are known to fail to duplicate real building behaviour because of lack of similitude. Advances in numerical analysis methods such as the finite element method are notable, but the analyses insufficiently duplicate the behaviour of structures to collapse, which involves significant material and kinematical non-linearity. For these reasons, the need for real data obtained by experiments with real-scale structures is extremely urgent for the advancement of earthquake engineering. E-Defense has been designed to meet this need.

2.1.1 LITERATURE REVIEW

developed a manual shake table using laminar box. However, it does not take into account pay load and the criterion for initiation of liquefaction in terms of CSR studied liquefaction behaviour of silty sand by conducting shake table tests on samples with different silt contents. The work focused mainly on resistance offered by silty sand to liquefaction for steady state of vibrations. Singh et al (2008) presented the liquefaction behaviour of the Solani sand by performing shake table tests at varying acceleration with constant frequency. The results were interpreted in terms of the pore water pressure and the time elapsed during various stages. It was observed that there was little effect of level of acceleration on the magnitude of maximum pore water pressure; however, time required in reaching the peak value decreased at higher acceleration.

The 20x20 ft shaking table at the Earthquake Engineering Research Center in Berkeley (EERC) is tested for interaction effects. The tests include three. Loading configurations: a bare table, a table loaded with 70 kips mass and a Table loaded with 68 kips single degree of freedom structure with a height of 219 inches. The shaking table has 5 degrees of freedom, one horizontal, one. vertical and 3 rotational degrees of freedom. When loaded with heavy and tall structures, the shaking table undergoes pitching (rocking) motion even.

This is mainly due to the flexibility in the pitch degree of freedom. It is observed that the interaction effects. are negligible for the bare table and the table with rigid mass case. In the case of the tall and heavy structure the pitching of the seismic simulator was evident when using a table horizontal command signal, In addition, a change in the frequency component of the horizontal table motion near the Structural frequency was observed. These include a shaking table with a horizontal actuator, a pitching actuator and a passive pitch stabilizer. Simplified spring-mass-damper models are also discussed. Methods for Avoiding modeling of the table flexibilities are presented. These include the Use of a two-directional base input motion and the simpler uni-directional effective base motion. Interaction effects are studied using response spectra. and the equivalent single degree of freedom table-structure system. It is concluded that the interaction effects are similar to those encountered in soil structure interaction studies. The interaction causes a reduction in the structural frequency and usually, but not always, an increase in damping. The change in the frequency component of the command signal Near the structural frequency due to interaction does not significantly affect. The ability of the shaking table to produce damaging motions to the test structure.Shaking table pitching and interaction effects were traditionally dealt with. by adding two vertical springs to the mathematical model to represent the Pitching flexibility. The passive stabilizer system was added to the EERC table in 1977 to reduce the flexibility in the pitching degree of freedom. For this reason, springs in the mathematical model used by Tang [2] are different from the ones used by later researchers. The required pro properties of the springs were typically derived from trial-and-error analysis, so that the coupled frequency structure matches the measured frequency. This approach, though convenient, can lead to serious errors because the springs will hide other modeling errors. The performance of shaking tables was the subject of several researchers at D.C. Berkeley in the past. Rea et al. [7] tested a small unidirectional Shaking table and the EERC table. Mathematical models were formulated to represent these shaking tables; however the models did not include the pitch effects. Rea found that: "...The magnitudes of the peak and notch distortions in the frequency Response of shaking tables are sensitive to the amount of force feedback employed by the control system.

In addition, the magnitudes depend on the ratio of the mass of the structure to the mass of the shaking table, and to the transmissibility function of the structure with respect to the table. Although the peak and notch effect may cause difficulties in determining the frequency response of structures by means of shaking tables, it has little effect on the accuracy to which a shaking table can reproduce earthquake-type motions... " also studied the effect of foundation compliance on a shaking table frequency response and found that foundation compliance affects the frequency response of the EERC shaking table only at low frequencies, and that the magnitude of the effect depends on the transmissibility function of the foundation with respect to the table. Blondet et al. performed a similar study on the unidirectional shaking table at the Catholic University of Peru [8]. In addition to Rea's model, a two Degree of freedom mass-spring-damper system was used to simulate the shaking table-structure interaction. Blondet et al. concluded the following[4].

1. The main aspects of the interaction problem can be studied from a mechanical viewpoint using a 2DOF spring-mass-damper system.

2. The interaction effects are mainly manifested by a peak and notch in the amplitude frequency response with the maximum attenuation occurring precisely at the natural vibration frequency of the test structure. This is particularly undesirable since the purpose of earthquake Simulation tests are to excite the structure at its own frequency in order to cause damage.

2.1.2 RESEARCH OBJECTIVES

The objective of this research project was to evaluate the EERC shaking table performance and to establish analytical models for the shaking table that can be used to account for and predict the shaking table-structure interaction effects. More specifically the objectives can be stated as:

1. to evaluate the table reproduction of typical earthquake records and to study the effects of the pitch motion on the structural response.

2. to establish a simplified mass-spring-damper system that can account for shaking table-structure interaction effects and can be easily incorporated in analytical models of the test structures; also, to devise ways for identifying the model parameters.

3. to develop an analytical model for a unidirectional shaking table system that includes feedback control loops.

4. to extend the mathematical model to include table pitching effects by means of

a. a mass-spring-damper system (hybrid model), and

b. a feedback control loop similar to that of the horizontal actuators;(Such models can be used to predict table performance and stability.)

5. to investigate ways of improving system performance through

6. modification of the command signal, the addition of actuators,etc.;and

7. to study methods of analyzing tested structures on the shaking table, which may avoid dealing with interaction altogether.

EARTHQUAKE SIMULATOR

The Earthquake Engineering Research Center (EERC) earthquake simulator consists of a 20 ft by 20 ft reinforced concrete platform. The table is a One-foot-thick reinforced concrete slab stiffened by heavy central transverse ribs at the bottom. The weight of the slab is about 100,000 lb. The slab is designed to have a fundamental vibration frequency above 20 Hz, so that it can be considered rigid within the usual operating frequency range (0-10Hz) of the shaking table.

At the time of the test, the EERC table could be programmed to produce a Specified vertical and a horizontal component of motion. The table, however, it has additional flexibility in the pitch, roll and twist directions. The shaking table is supported vertically by 4 active actuators located in a square pattern, 12 ft apart; Four passive actuators, in a 17-ft square pattern, were added in the late seventies to reduce the flexibility in the pitch degree of freedom and to increase the overturning moment capacity. The horizontal Motion is produced by three active actuators. Figure 2.1 shows a sketch of the table with the locations of actuators. Figure 2.2 shows a schematic of the hydraulic interconnection of the passive pitch stabilizers. The actuator

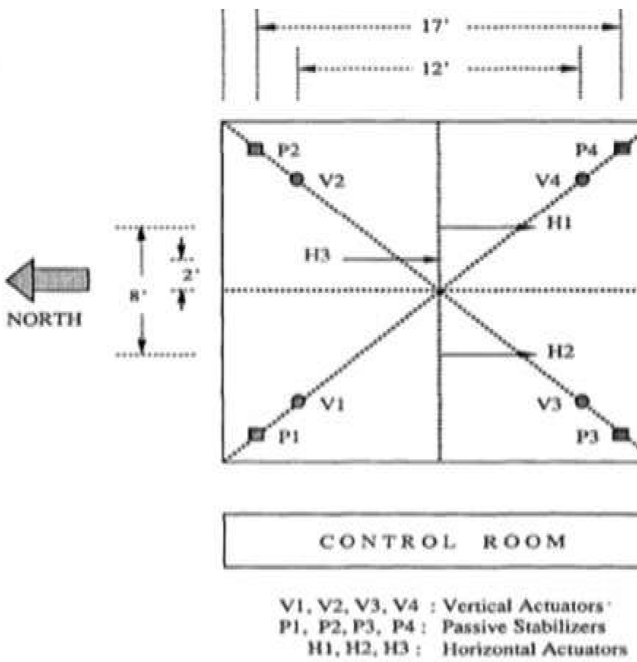

Fig 2.1: Actuator locations in Erec earthquake

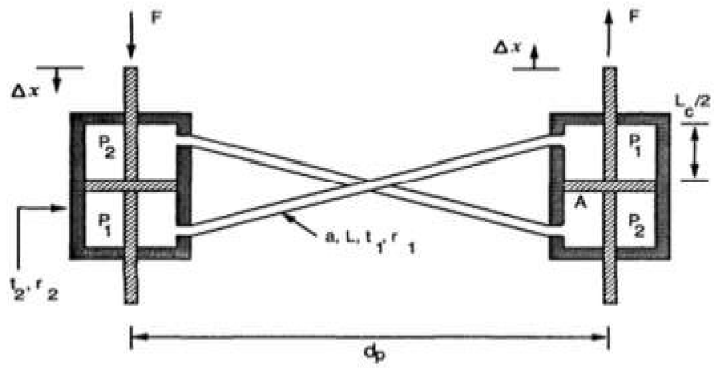

Fig 2.2: hydraulic passive stabilizer unit

Capacities are 25,000 lb. for each vertical actuator and 70,000 lb. for each horizontal actuator. The horizontal actuators have 170 g pm (gal/min) servo valves; The vertical actuators have 90 g pm servo valves.

Table 2.1: Specifications for MTS actuators used in Erec earthquake simulator

ACTUATOR (as in Fig. 2.1)	MODEL NUM.	AREA (in^2)	STROKE (in)	SERVOVALVE (MODEL #)	FLOW (gpm) CAPACITY	CAPACITY (kips)
H1	204.32	25.4	12	251.42	170	50
H2	204.32	25.4	12	251.42	170	50
H3	204.32	25.4	12	251.42	170	50
V1	204.25	9.6	4	251.32	90	25
V2	204.25	9.6	4	251.32	90	25
V3	204.25	9.6	4	251.32	90	25
V4	204.25	9.6	4	251.32	90	25
P1	204.72	26.0	4	N/A	N/A	50
P2	204.72	26.0	4	N/A	N/A	50
P3	204.72	26.0	4	N/A	N/A	50
P4	204.72	26.0	4	N/A	N/A	50

The Specifications for the various EERC shaking table actuators. The two translational degrees of freedom can be programmed to produce Any type of wave form within the limits of the displacement, velocity and force capacity and the frequency bandwidth of the table. With these capacities, the table is able to produce motions about twice those recorded during the EI Centro earthquake of 1940, including both the N-S horizontal, and the vertical components combined. The displacement is limited by the actuator stroke and the table clearance, +_ 5 inches in the horizontal and +_ 2 inches in the vertical directions. The flow rate in the servo valves limits the Maximum velocities produced in the horizontal and vertical directions to 25 in/sec and 15 in/sec,

respectively. The maximum acceleration is limited by the force limits of the actuators together with the mass of the table structure system. Figure 2.3 shows the acceleration limits for the unloaded table as a function of frequency.

Table 2.2 identification of test channels

CHANNEL ID	CHANNEL NAME	FULL NAME	UNITS
1	avg hdisp	Average Horizontal Displacement	inches
2	avg vdisp	Average Vertical Displacement	inches
3	avg hacc	Average Horizontal Acceleration	G
4	avg vacc	Average Vertical Acceleration	G
5	pitch acc	Pitch Acceleration	rad/sec2
6	roll acc	Roll Acceleration	rad/sec2
7	twist acc	Twist Acceleration	rad/sec2
8	v2 disp	V2 Vertical Actuator Displacement	inches
9	v3 disp	V3 Vertical Actuator Displacement	inches
10	v4 disp	V4 Vertical Actuator Displacement	inches
11	h span	Command Displacement	inches
12	h1 force	H1 Horizontal Actuator Force	kips
13	h2 force	H2 Horizontal Actuator Force	kips
14	h3 force	H3 Horizontal Actuator Force	kips
15	v1 force	V1 Vertical Actuator Force	kips
16	v2 force	V2 Vertical Actuator Force	kips
17	v3 force	V3 Vertical Actuator Force	kips
18	v4 force	V4 Vertical Actuator Force	kips
19	h1 disp	H1 Horizontal Actuator Displacement	inches
20	h2 disp	H2 Horizontal Actuator Displacement	inches
21	p1 stab	P1 Passive Stabilizer Force	kips
22	p2 stab	P2 Passive Stabilizer Force	kips
23	p3 stap	P3 Passive Stabilizer Force	kips
24	p4 stab	P4 Passive Stabilizer Force	kips
25	h vel	Table Horizontal Velocity	in/sec
26	accN-NE	Accelerometer	G
27	accN-NW	Accelerometer	G
28	accW-NW	Accelerometer	G
29	accW-SW	Accelerometer	G
30	potN-SW	Potentiometer	inches
31	potN-SE	Potentiometer	inches
32	accCMD	Accelerometer	G

During operation, the air in the pit beneath the shaking table is pressurized so that the total weight of the table and the structure being tested is balanced by the difference between the air pressure in the pit and the ambient air pressure. The pit entrance is sealed by two airtight doors that provide a lock chamber and thus permit access to the pit while the air in the pit is pressurized. The one-foot horizontal gap between the edge of the table and the interior foundation walls are sealed by a 24-inch-wide strip of vinyl covered nylon fabric. A differential air pressure of 1.55 psi is required to balance the weight of the shaking table alone. Oil at 3,000 psi is supplied by four 90 g pm pressure regulated pumps, each of which is driven by a 120 hp electric motor. Accumulators that can double the peak instantaneous flow rates are installed in the main oil line, but the Oil supply is not sufficient to produce maximum

horizontal and vertical velocities simultaneously. However, it is considered unlikely that the maximum Horizontal and vertical components of an earthquake would occur simultaneously.

The actuator forces are reacted by a massive foundation block, which is a Reinforced concrete structure in the form of an open box with 5 ft thick sides. sides. The outside dimensions of the box are 32 x 32 x 15 ft, and the inside Dimensions are 22 x 22 x 10 ft. The foundation weighs 1,580,000 lbs. Specifications of the shaking table are given in Table 2.2

Plan dimensions	20 x 20 ft (6.1 x 6.1 meters)
Model tie down locations	2-inch diameter holes @ 36 inches on center (914 mm)
Model weight capacity	130,000 lb (578 KN)
Overhead clearance	40 ft to ceiling (12.2 meters) 32 ft to 10 ton crane (9.75 meters)
Overturning resistance	3,343 kip-ft (229 NM)
Displacement	Horizontal ∓ 5 inches (∓ 152 mm) Vertical ∓ 2 inches (∓ 76 mm)
Velocity	Horizontal ∓ 25 ips (∓ 635 mm/sec) Vertical ∓ 15 ips (∓ 381 mm/sec)
Acceleration	Horizontal ∓ 1.5 G (∓ 1472 gal) Vertical ∓ 1.0 G (∓ 981 gal)
Bandwidth	0 - 20 Hz

Table 2.3:specifications of EERS shaking table

DATA ACQUISITION SYSTEM

The data acquisition system can acquire up to 128 data channels. An analogue to digital converter converts the filtered data into digital form to be stored and processed by a VAX 11/750 computer. Data analysis and display are mainly done through the S Statistical Software available on VAX. The data acquisition system samples data at 50 KHZ, and when acquiring data on all 128 channels, The maximum sampling rate per channel is 50,000/128 = 390 samples per second. During the current tests an analog lowpass filter With cut-off frequency of 100 Hz was applied to all output channels before they were digitized. Sampling was normally done at twice the filter frequency in order to avoid aliasing in the digitized signals. Aliasing is a phenomenon that occurs when sampling a high frequency signal at a sampling rate less than twice that frequency. Undersampling would cause the Digitized signal to have lower frequency signals generated from the high frequency data. It is usually very difficult to get rid of these aliased frequencies. Once the data is collected, simple filtering would not help in this case

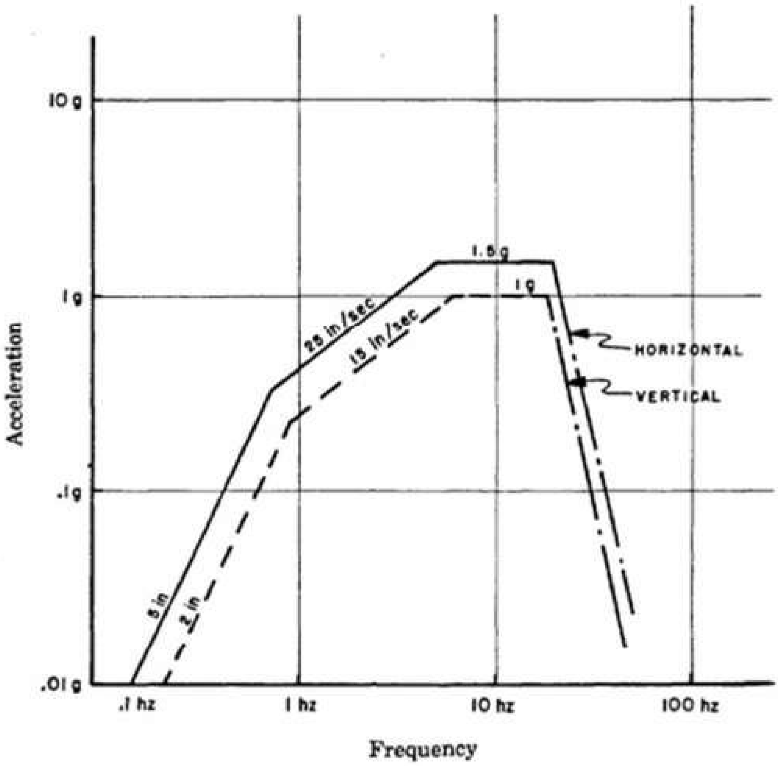

Fig. 2.3: EERC Shaking Table Motion Limits. Bare Table.

TEST STRUCTURE

Figure 2.4 shows the single degree-of-freedom structure mounted on the EERC shaking table in tests performed for this investigation. The structure It is a four story, braced steel frame weighing 6.45 kips and supporting a weight of 62.5 kips. This test frame is the lower part of the steel frame Tested by Hucklebridge [3].

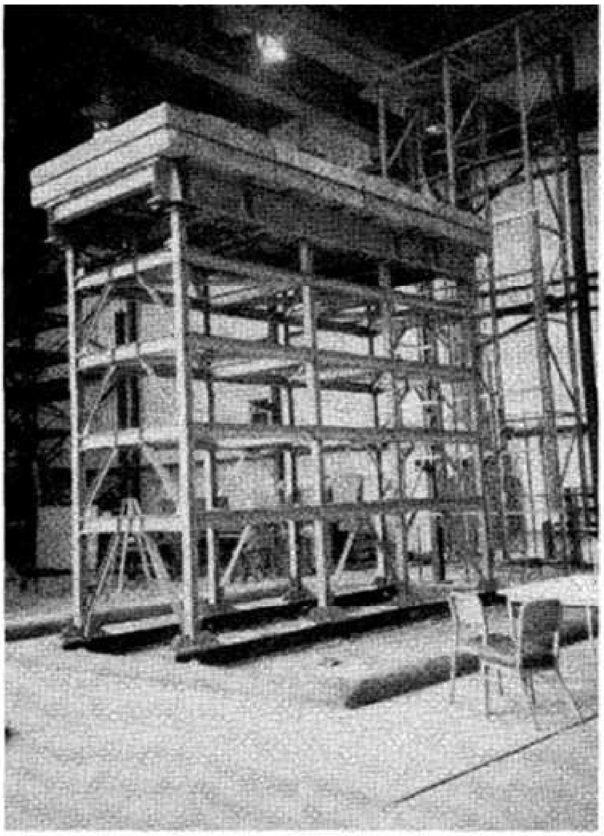

Fig. 2.4: SDOF Structure Mounted on EERC Shaking Table.

The structure consists mainly of W6x8.5 beams and W4x13 steel columns. A W8x31 base beam connects it to the shaking table by means of prestressed steel rods spaced at 3 ft intervals which pass through 2-in diameter Holes in the I-ft thick reinforced-concrete table. The two identical parallel Frames that form the steel structure are spaced 6 ft apart, and the total Length of the frame in the test direction is 18 ft. The height of the first floor is 4 ft above the base beam; All the other floors are 3-ft high except for the top floor. That floor consists of 1.5-ft high columns supporting 16-inch-deep beams, on which are placed eight concrete blocks weighing 4 kips each. The height of the concrete blocks is 15 inches. The concrete blocks support 26.4 kips of lead blocks. The center of mass of the lead blocks is 11 inches above the upper face of the concrete blocks.

A sketch of the instrumentation is shown in Fig. 2.5. Four accelerometers at the top of the structure were attached to the top deep beams to measure the structure responds -- two sensing motion in the direction of the table movement and two oriented to indicate accelerations perpendicular to the table motion. The accelerometers were 189.3 inches above the top face of the shaking table. Two displacement meters were also used in the lateral direction (direction of table motion), and the displacements were measured with respect to a reference frame which was supported on the laboratory floor away from the table.

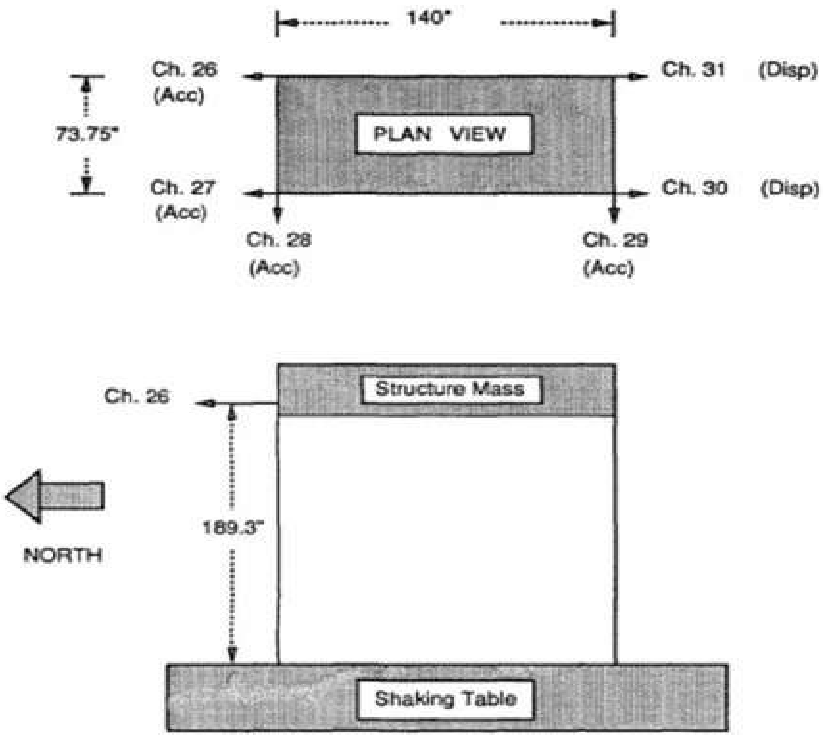

Fig. 2.5: Locations of accelerometers and displacement meters.

TEST MASS

The table was loaded with three concrete blocks (WxHxL=48x21.5x240inches) having a total weight of 70.5 kips. Each block was anchored to the table by post-tensioned steel rods. The long direction of the blocks was aligned perpendicular to the horizontal direction of shaking. This total Mass was used to determine the effect on the table performance of a rigid Test specimen with relatively low overturning moment. The center of gravity of the mass was only 10.75 inches above the table surface, as shown in Fig. 2.6

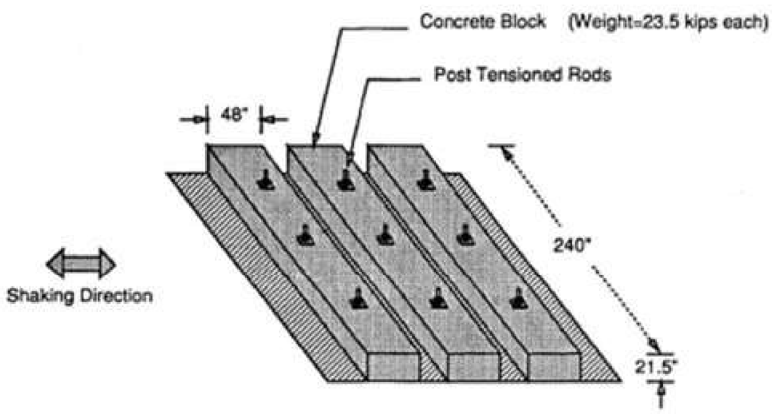

Fig. 2.6: Concrete blocks on EERC shaking table.

Chapter 3
Mechanical Design

3.1.1 Overview.

In this Section we will go through the mechanical design, drawings and the materials used to achieve the desired strength, and information aboutthe material used, With stress, strain, displacement analysis of the project.

3.1.2 <u>Design Assembly 3D Model.</u>

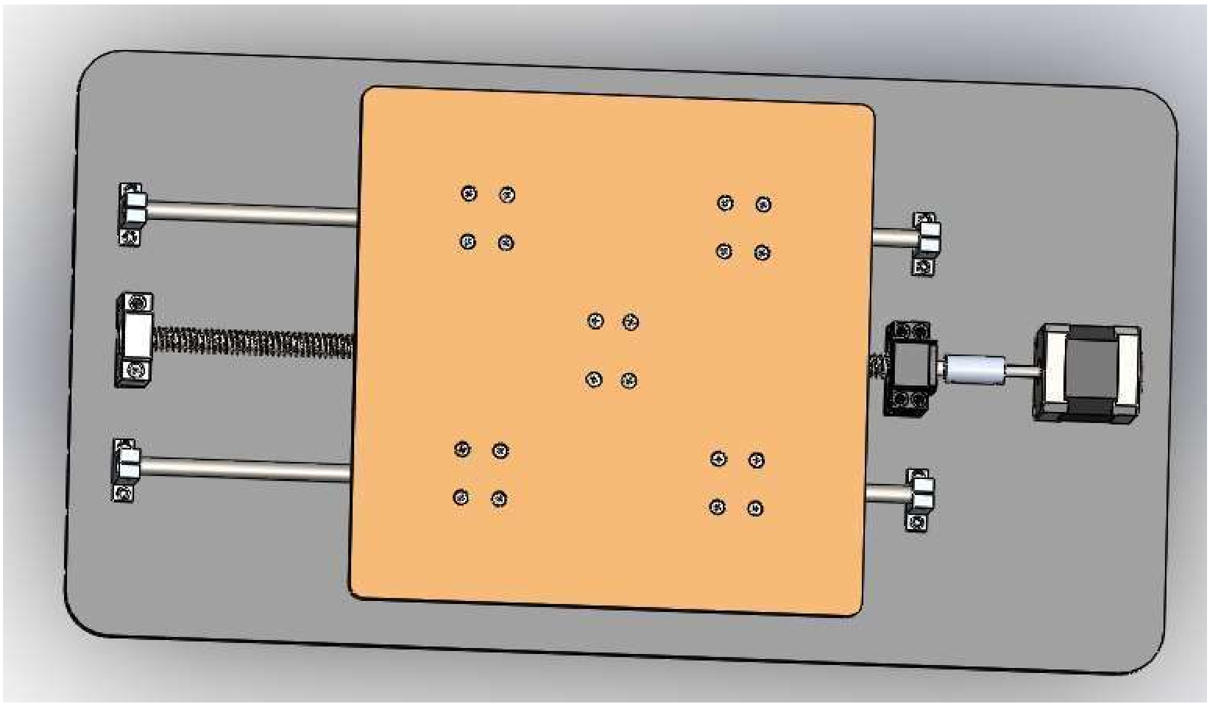

Fig. 3.1 design assembly 3D model

3.1.3 <u>Assembly Parts</u>

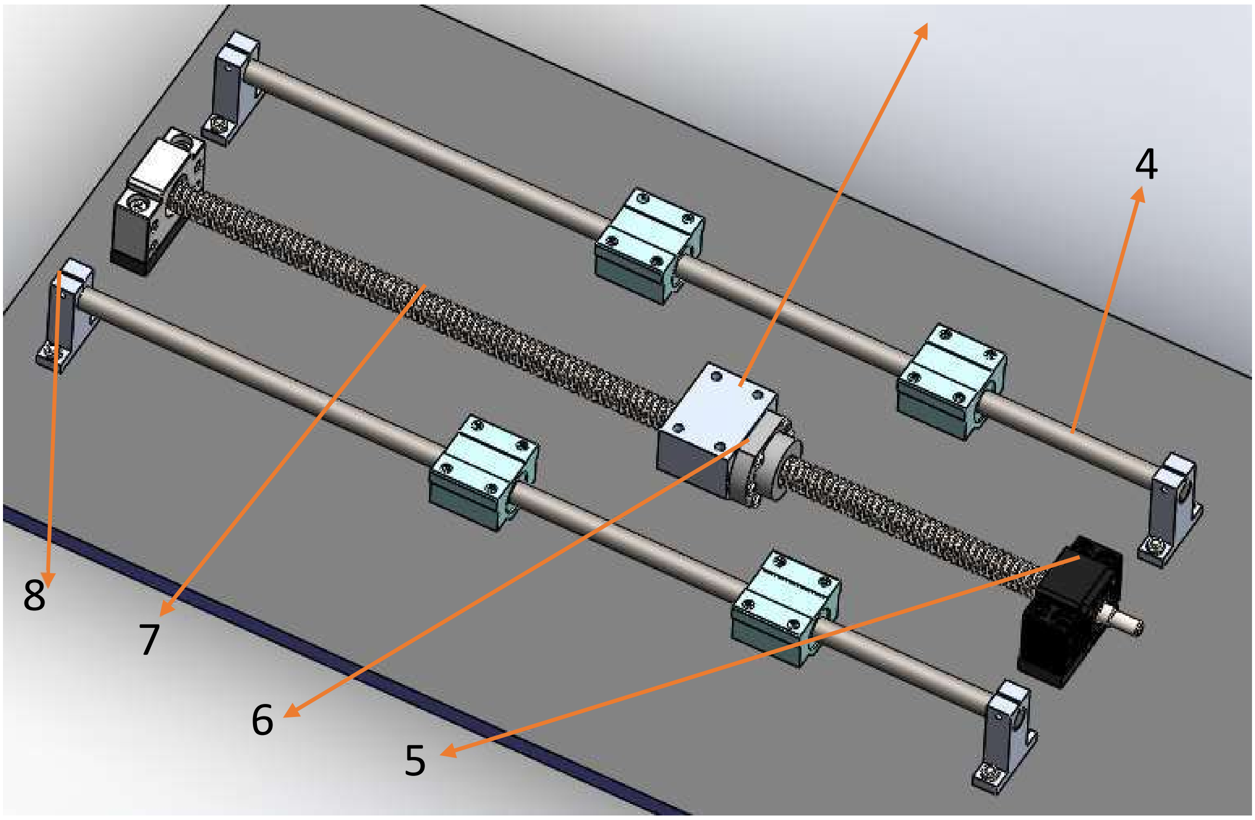

Fig. 3.2(a) Assembly Parts

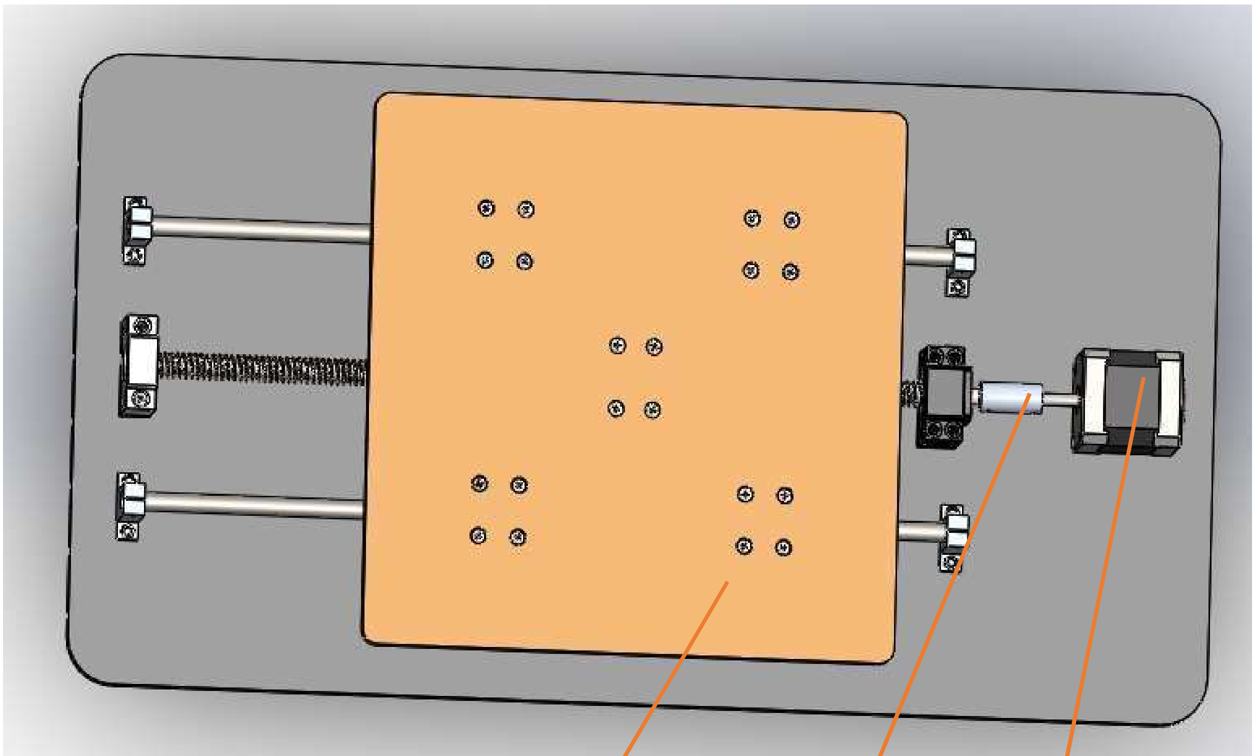

Fig. 3.2(b) Assembly Parts

NO.	PART NUMBER	MATERIAL	QTY.
1	Base Plate	Balsa	1
2	Linear Motion Ball Slide Bearings	Carbon steel	4
3	lead Screw Nut Seat Bracket Holder Mount Housing	Carbon steel	1
4	guide shafts.	Steel 1.1213	2
5	Lead Screw End Supports	Carbon steel	2
6	**Lead** nut		1
7	Lead screw.	304 Stainless Steel.	1
8	**Linear Rail Shaft Support**	Carbon steel	4
9	Table	Balsa	1
10	Flex Coupling	Aluminium Stainless Steel	1
11	motor		1

Table 3.1. Assembly Parts

3.1.4 **Lead screws**

The Lead screws (also known as translation screws) are used to convert rotary motion into translatory motion. For example, in the case of the lead screw of lathe, the rotary motion is available, but the tool has to be advanced in the direction of the cut against the cutting resistance of the material. In case of screw jack, a small force applied in the horizontal plane is used to raise or lower a large load. Power screws are also used in vices, testing machines, presses, etc. In most of the power screws, the nut has axial motion against the resisting axial force while the screw rotates in its bearings. In some screws, the screw rotates and moves axially against the resisting force while the nut is stationary and in others the nut rotates while the screw moves axially with no rotation [5]

3.1.5 Types of Screw Threads used for Lead screws.

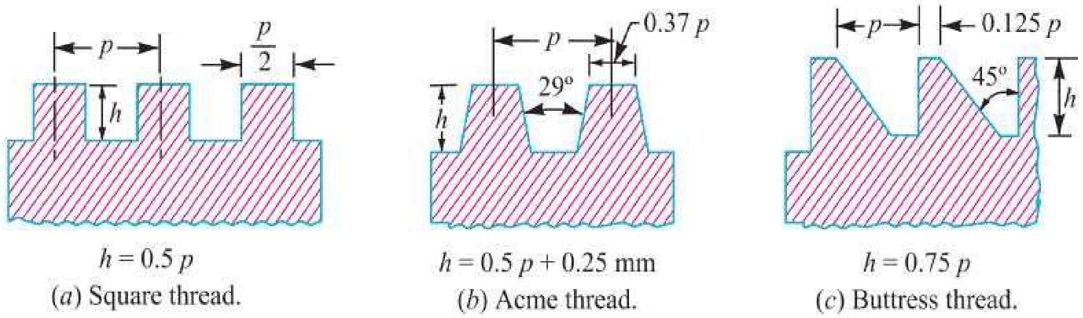

Fig. 3.3 Types of Screw Threads

(i) **Square thread**: A square thread, as shown in Fig. 3.3 (a), is adapted for the transmission of power in either direction. This thread results in maximum efficiency and minimum radial or bursting

(ii) Acme or trapezoidal thread.

An acme or trapezoidal thread, as shown in Fig. 3.3 (b), is a modification of square thread. The slight slope given to its sides lowers the efficiency slightly than square thread and it also introduce some bursting pressure on the nut, but increases its area in shear. It is used where a split nut is required and where provision is made to take up wear as in the lead screw of a lathe.

(iii) Buttress thread.

A buttress thread, as shown in Fig. 3.3 (c), is used when large forces act along the screw axis in one direction only. This thread combines the higher efficiency of square thread and the ease of cutting and the adaptability to a split nut of acme thread. It is stronger than other threads because of the greater thickness at the base of the thread. The buttress thread has limited use for power transmission. It is employed as the thread for light jack screws and vices.

In our project, we utilize ACME screws as a crucial component. ACME screws are trapezoidal screw threads that offer robustness, high load-bearing capacity, and efficient torque transmission. These threads are commonly employed in applications involving power transmission and linear motion systems.

The implementation of ACME screws in our project provides several advantages. The trapezoidal thread profile enhances the strength and durability of the screws, enabling them to withstand heavy loads and resist wear over time. Additionally, ACME screws offer superior efficiency in converting rotational motion into linear motion, making them ideal for our project.

ACME Screw Design: ACME screws have a trapezoidal thread profile with a 29-degree thread angle. The thread shape features flattened crests and roots, which improves load distribution and enhances the screw's strength. The design of ACME screws allows for efficient power transmission and high load-bearing capacity.

ACME Screw Materials: ACME screws are typically made from materials that provide high strength and wear resistance. Common materials include stainless steel, alloy steel, and hardened steel. The choice of material depends on factors such as the application requirements, environmental conditions, and desired longevity.

Versatile Applications: ACME screws find applications in various industries, including manufacturing, robotics, automotive, aerospace, and construction. They are commonly used in power transmission systems, lifting mechanisms, positioning stages, clamping devices, and other linear motion applications.

Thread Specifications: ACME threads are defined by parameters such as major diameter, pitch, and thread depth. These values determine the size and geometry of the thread. In the following standard table 3.2

Nominal or major diameter (d) mm.	*Minor or core diameter (d_c) mm*	*Pitch (p) mm*	*Area of core (A_c) mm^2*
10	6.5	3	33
12	8.5		57
14	9.5		71
16	11.5	4	105
18	13.5		143
20	15.5		189

table 3.2- Thread Specifications

3.1.6 Force Calculations of Power Screws

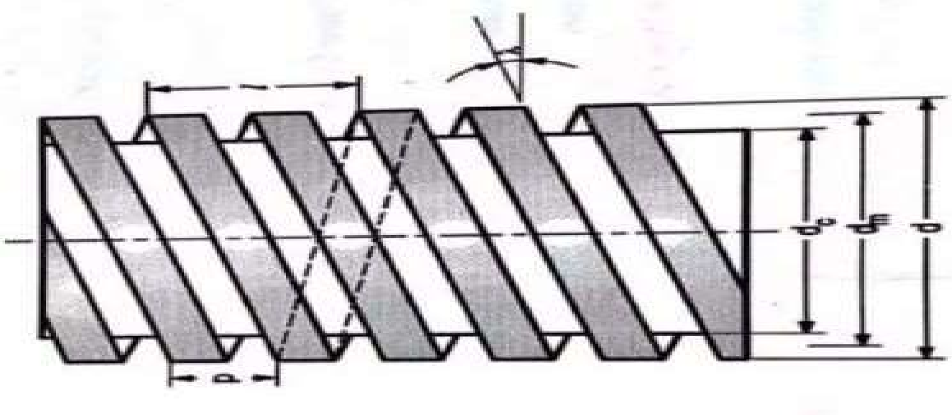

Fig. 3.4 Power Screws

(iv) Nominal Diameter (d):

It is the largest diameter of an external or internal thread. The screw is specified by this diameter. It is also known as outer diameter or major diameter.

(v) Core Diameter (dc):

It is the smallest diameter of an external or internal thread. It is also known as inner diameter or root diameter.

(vi) Mean Diameter (dm):

It is the average nominal diameter and the core diameter.

It is also known as pitch diameter.

(vii) 4.Pitch(p):

It is the distance from any point on the thread to the corresponding point on the adjacent thread, measured parallel to the axis.

(viii) lead(I):

It is the distance which a screw advances axially in one rotation of the nut. It may also be defined as the distance between two corresponding points on the same helix.

(i) Lead Angle (α):

It is an angle made by a helix or a thread with a plane perpendicular to an axis of screw.

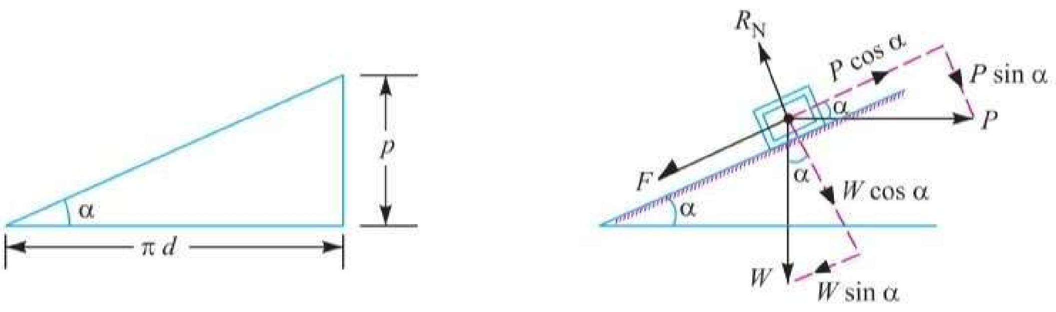

(a) Development of a screw.   (b) Forces acting on the screw.

Fig.3.5

P $\cos\alpha = W\ sin\alpha + \ \mu(Psin\ \alpha + Wcos\ \alpha)$

$= \ W\ sin\alpha + \ \mu Psin\ \alpha + \mu Wcos\ \alpha)$

P $\cos\alpha$ - $\mu Psin\ \alpha$ = $W\ sin\alpha$ + $\mu Wcos\ \alpha$

P ($\cos\alpha$ - $\mu sin\ \alpha$) = $W\ (sin\alpha + \mu cos\ \alpha)$

P = W $\times \frac{(sin\alpha\ +\mu cos\ \alpha)}{((\cos\alpha\ -\ \mu sin\ \alpha))}$

Or

P = W tan $(\alpha + \emptyset)$ =W$(\frac{tan\ \alpha+tan\ \emptyset}{1-tan\ \alpha\ tan\ \emptyset})$

$\mu = \ tan\ \emptyset = 0.05,$ $\qquad tan\ \alpha = \frac{p}{\pi d} = \frac{4}{\pi\times16} = 0.079$

P = W $\times$ $(\frac{tan\ \alpha+tan\ \emptyset}{1-tan\ \alpha\ tan\ \emptyset}) = 98.1 \times [\frac{0.079\ -0.05}{1-0.079\times0.05}]$ = 2.86N

Calculate the Load Torque *TL*

Load Torque $T_L = \frac{F\ .\ P_B}{2\pi\eta} + \frac{\mu .F_0}{2\pi}$

F = Force of moving direction
F_o= Pilot pressure weight ($\frac{1}{3}$F) =2.59N
μ = Internal friction coefficient of pilot pressure nut
η = Efficiency (0.85 to 0.95)
P_B = Lead screw pitch = 4mm
F_A = External force = 2.86N

$\text{F} = \boldsymbol{F_A + m.g(sin\theta + \mu.cos\theta)}$

F= 2.86 + 10× 9.81(sin 0 + 0.05 cos 0)= 7.765 N

$\boldsymbol{T_L = \frac{7.765 \times 4\times10^{-3}}{2\pi\times0.9} + \frac{0.05 \times 2.59 \times 4\times10^{-3}}{2\pi}}$ **= 0.0558 N.cm**

Calculate the Acceleration Torque *Ta*

$\boldsymbol{T_a = J_{total} \times \alpha}$

Inertia of Lead Screw $\boldsymbol{J_B = \frac{\pi}{32} . \rho . L_B . D_B{}^4}$

$\boldsymbol{\rho}$ Mass density of material:

Iron [density $\boldsymbol{\rho} =$ (7.9 × $\mathbf{10^{-3}}$kg /cm3)]

$\boldsymbol{L_B}$ Total length of lead screw: = 500mm

$\boldsymbol{D_B}$ lead screw shaft diameter: = 16mm

$\boldsymbol{J_B = \frac{\pi}{32} \times 7.9 \times 10^{-3} \times 500 \times 10^{-3} \times (16 \times 10^{-3})^4 = 2.776 \times 10^{-6}\ Km^2}$

Inertia of Table and work $J_T = (\frac{P_B}{2\pi})^2$

$\boldsymbol{= 10(\frac{4\times10^{-3}}{2\pi})^2 = 1.01\times 10^{-6}\ Km^2}$

Total Inertia $J_L = J_B + J_T$

$\boldsymbol{= 2.776 \times 10^{-6} + 1.01\times 10^{-6} = 3.786 \times 10^{-6}\ Km^2}$

$\boldsymbol{T_m = 0.0053 m.N + 0.146\ N.m \times 2 = 29.73\ N.cm}$

3.2 Study Analysis.

Stresses in Lead screws

A power screw must have adequate strength to withstand axial load and the applied torque. Following types of stresses are induced in the screw.

3.2.1 **tensile or compressive stress due to an axial load**. The direct stress due to the axial load may be determined by dividing the axial load (W) by the minimum cross-sectional area of the screw ($\boldsymbol{A_c}$) i.e. area corresponding to minor or core diameter ($\boldsymbol{d_c}$).

∴ Direct stress (tensile or compressive)

$$\boldsymbol{\sigma = \frac{W}{A_c} = \frac{98.1}{105} = 0.934\ N/mm^2}$$

This is only applicable when the axial load is compressive and the unsupported length of the screw between the load and the nut is short.

3.2.2 **Torsional shear stress.** Since the screw is subjected to a twisting moment, therefore torsional shear stress is induced. This is obtained by considering the minimum cross-section of the screw. We know that torque transmitted by the screw,

$$T = \frac{\pi}{16} \times \tau(d_c)^2$$

or shear stress induced,

$$\tau = \frac{16T}{\pi(d_c)^3}$$

Torque required of lead screw

$$T_1 = P \times \frac{d}{2}$$

$$\boldsymbol{T_1 = p \times \frac{d}{2} = 2.86 \times \frac{16 \times 10^{-3}}{2} = 0.02288\ N.}$$

$$\boldsymbol{\tau = \frac{16T}{\pi(d_c)^3} = \frac{16 \times 0.02288}{\pi(11.5 \times 10^{-3})^3} = 76618.4\ N.m}$$

When the screw is subjected to both direct stress and torsional shear stress, then the design must be based on maximum shear stress theory, according to which maximum shear stress on the minor diameter section,

$$\tau_{max} = \frac{1}{2}\sqrt{(\sigma_t or \sigma_c)^2 + 4\tau^2}$$

$$\tau_{max} = \frac{1}{2}\sqrt{(0.934)^2 + 4(76618.4)^2}$$

= 76618.4 MPa

Chapter 4
Methodology

4.1 Set up Machine.

1- Install the nut in lead screw as shown Fig 4.1

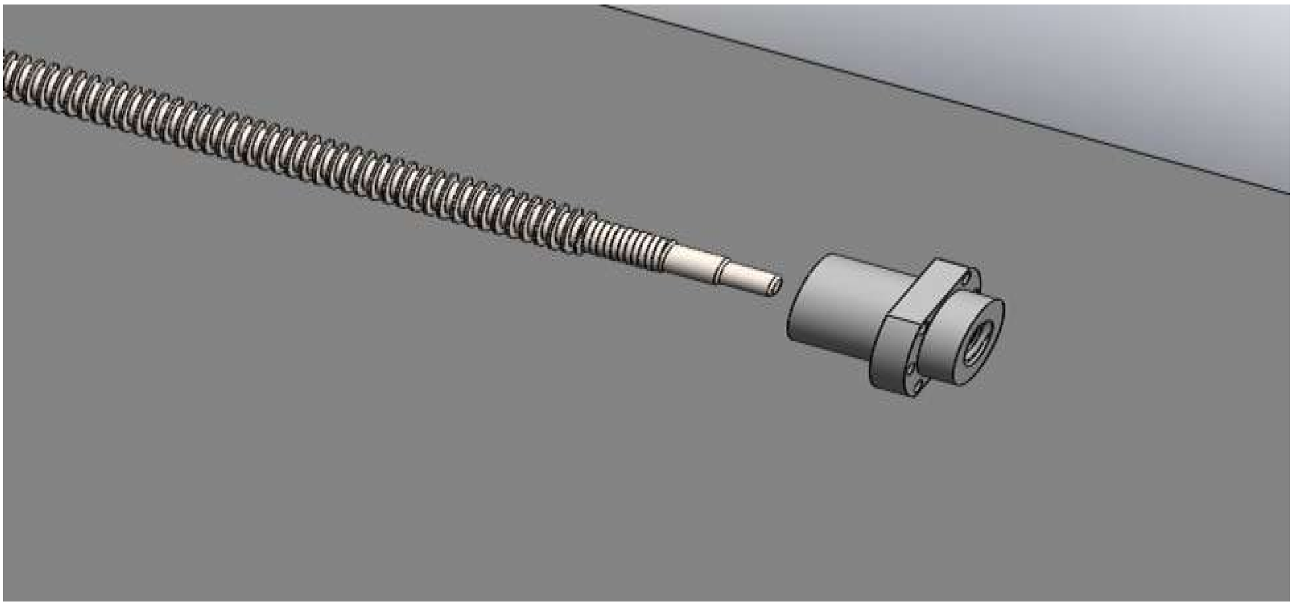

Fig 4.1- Install the nut in lead screw

2- install lead Screw Nut Seat Bracket Holder Mount Housing in lead screw as shown Fig 4.2

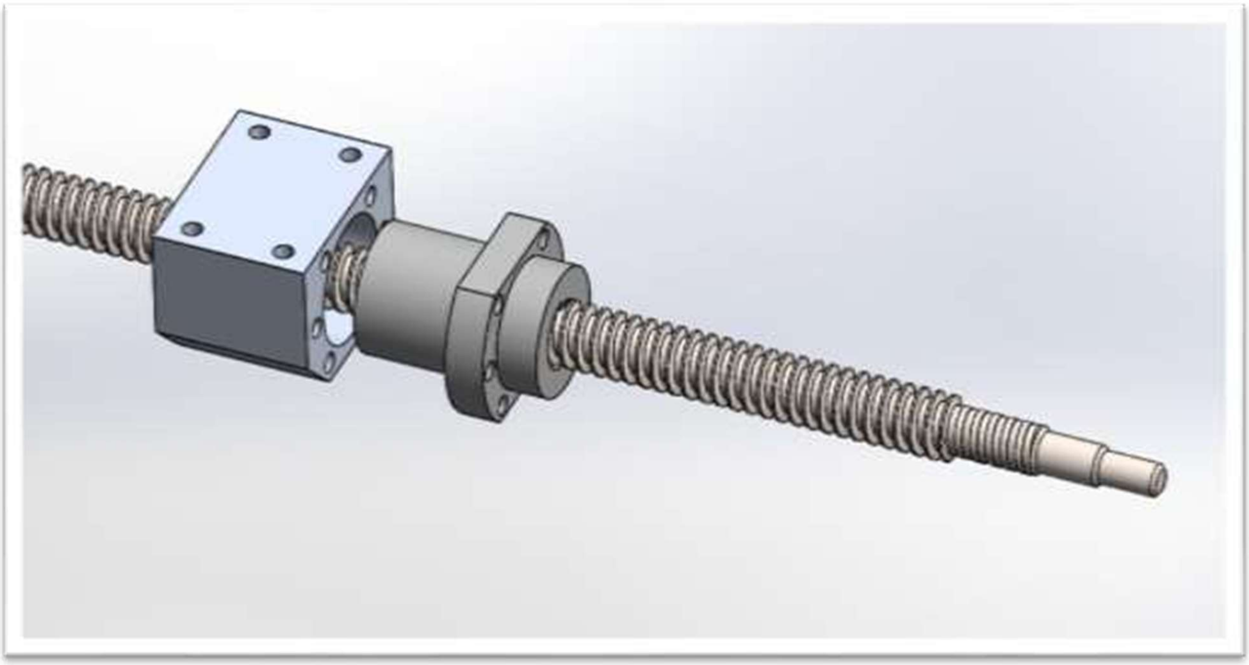

Fig 4.2 install lead Screw Nut Seat Bracket Holder Mount Housing in lead screw

3- install nut lead Screw Nut Seat Bracket Holder Mount Housing by using screws as shown Fig 4.3

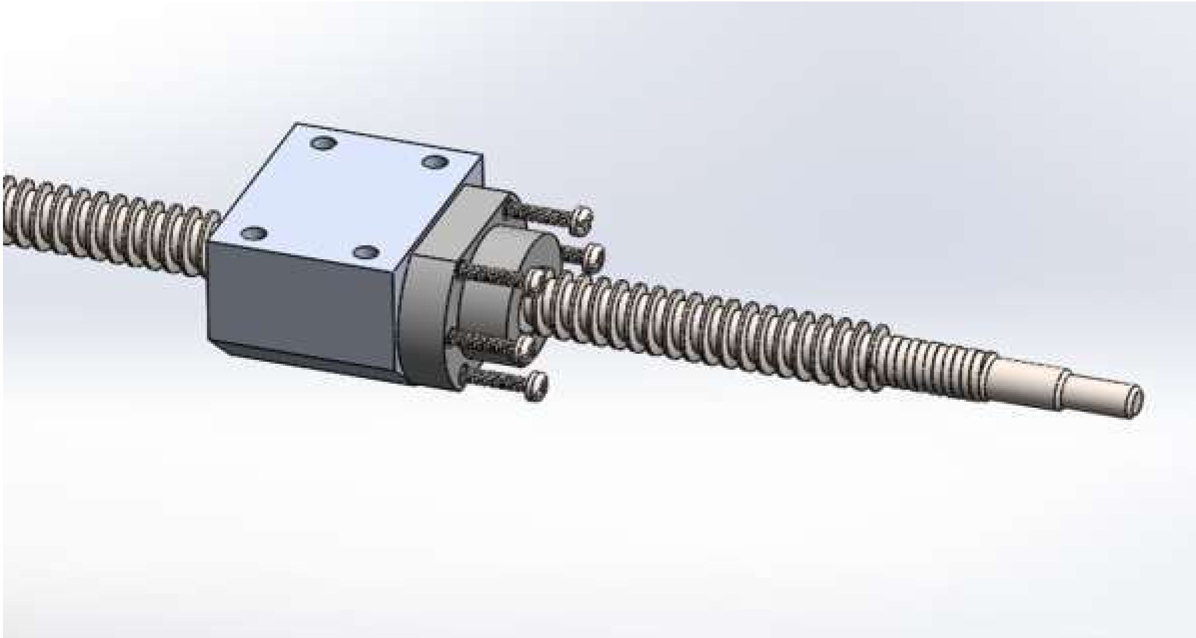

Fig 4.3- install nut lead Screw Nut Seat Bracket Holder Mount Housing by using screws.

4- install Lead Screw End Supports in lead screw as shown Fig 4.4

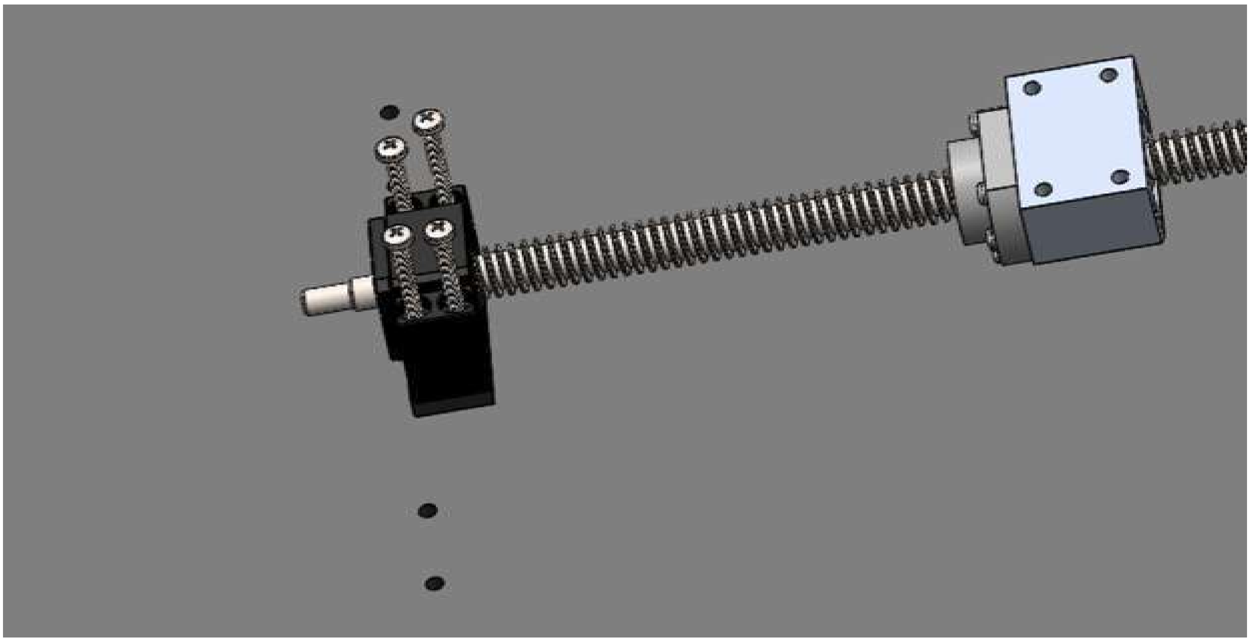

Fig 4.4 - install Lead Screw End Supports in lead screw

5- install Lead Screw End Supports in base plate as shown Fig 4.5

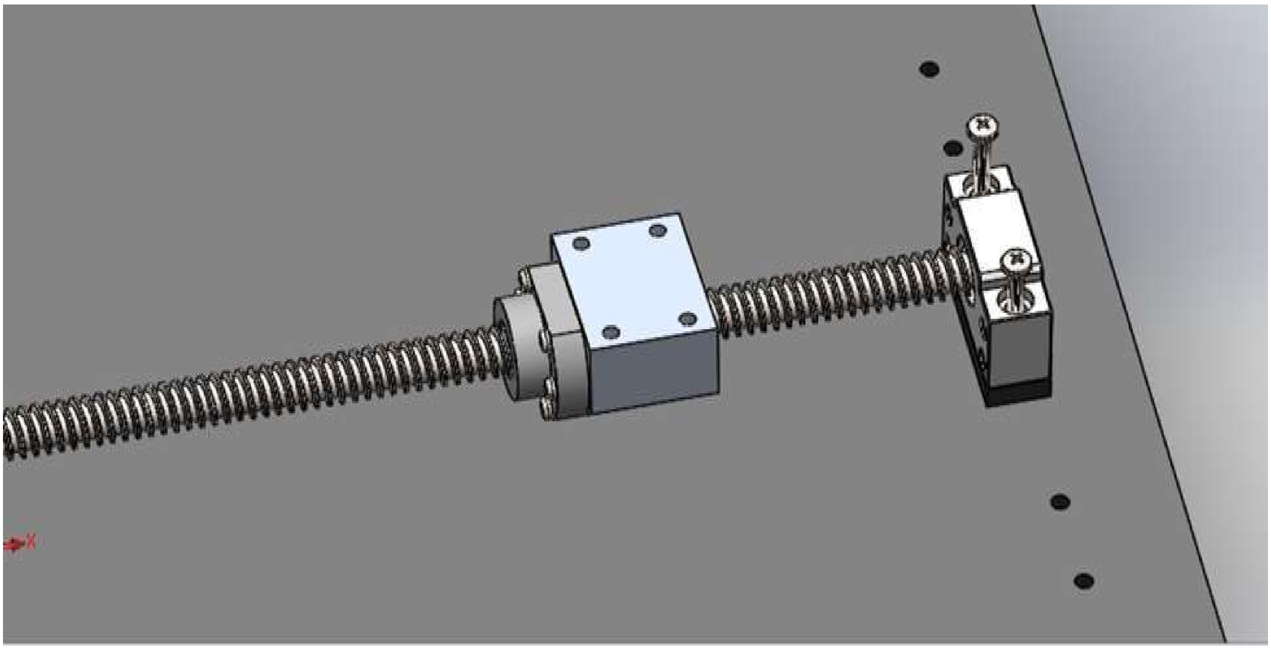

Fig4.5- install Lead Screw End Supports in base plate

6- install four Linear Rail Shaft Support in base plate, install in guide shafts and install guides shafts in Linear Rail Shaft Support as shown Fig 4.6

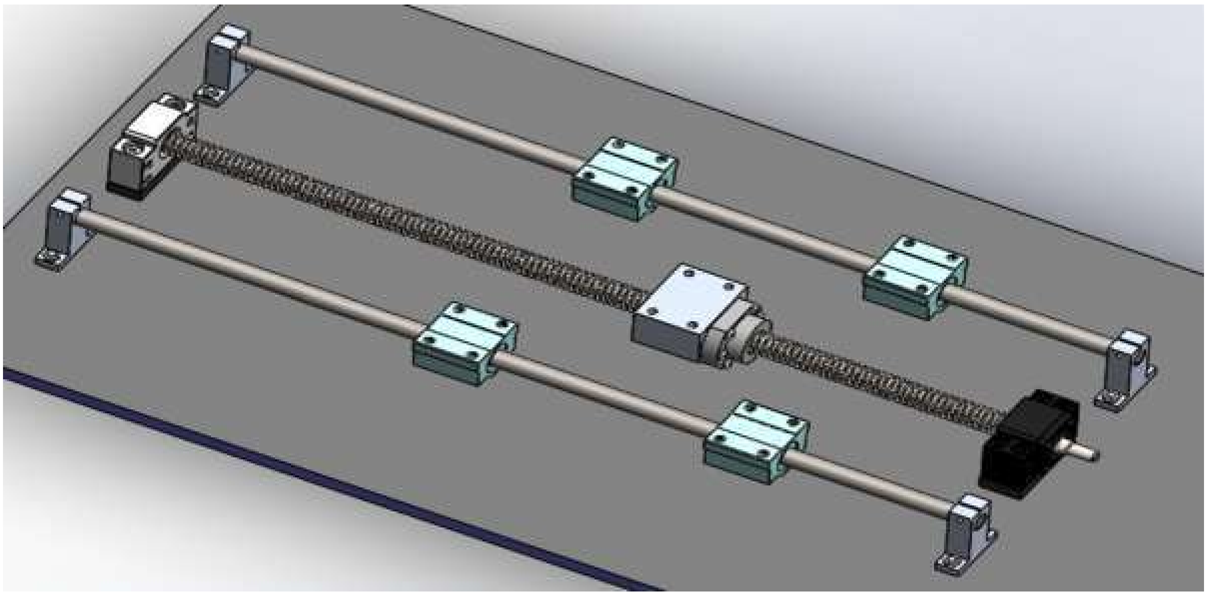

Fig 4.6- install four Linear Rail Shaft Support in base plate

10- install table in and lead Screw Nut Seat Bracket Holder Mount Housing by using screws as shown fig 4.7.

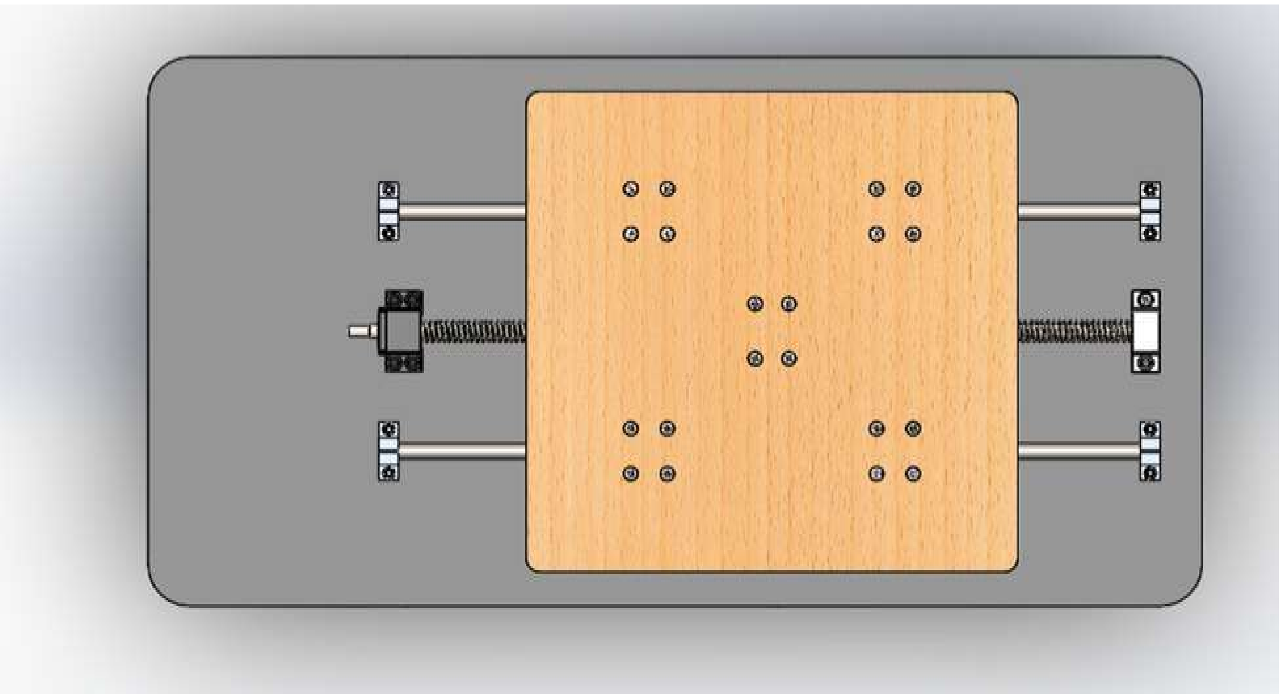

Fig 4.7- install table in and lead Screw Nut Seat Bracket Holder Mount Housing by using screws

11- install stepper motor in lead screw by using flex coupling as shown Fig 4.8

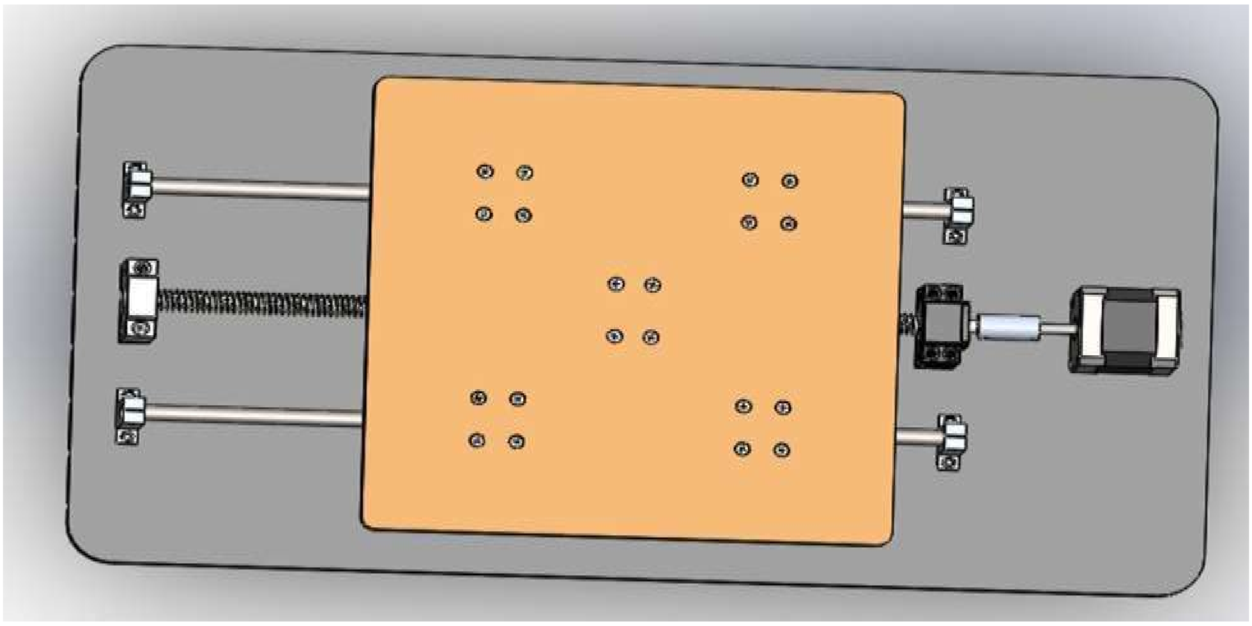

Fig 4.8- install stepper motor in lead screw by using flex coupling

Chapter 5
Electrical Design

5-1 _ electrical component

5-1-1_ ADXL345 sensor

Fig 5.1 ADXL345 sensor

The ADXL345 is well suited to measure the static acceleration of gravity in tilt-sensing applications, as well as dynamic acceleration resulting from motion or shock.

Its high resolution (4 mg/LSB) enables measurement of inclination changes less than 1.0.

Features

1) 2.0-3.6VDC

2) Supply Voltage

3) Ultra Low Power: 40uA in measurement mode, 0.1uA in standby 4)2.5V

5)Tap/Double Tap Detection

6) Free-Fall Detection

7) SPI and I2C interfaces

8)Dimensions: 21mm x 16mm

5-1-2- 5 DC MOTOR

Electrical Data

Rated Voltage	V	24
Max. Continuous Current	A	4.5
Max. Operating Voltage	V	36
Inductance	mH	2.0
K_t Torque Constant (± 10%)	oz-in/A [N-m/A]	8.9 [0.062]
K_v Voltage Constant (± 10%)	V/kRPM	6.5
Winding Resistance @ Ambient	Ohms	1.0

1-**Voltage Rating**: 24 VDC

2-**Power Rating**:

The power rating of a 24V DC motor can vary depending on the specific model and application, but the common range is from 50 watts to 500 watts.

3-**Speed Range:**

24V DC motors typically have a no-load speed range of approximately 1,000 to 5,000 RPM.

The actual speed of the motor will depend on the load applied and the motor's torque characteristics.

4-**Torque**:

24V DC motors can provide a wide range of torque output, usually from 0.1 Nm to 10 Nm or more, depending on the motor size and design.

The torque output will decrease as the motor speed increases.

5-**Efficiency:**

The efficiency of a 24V DC motor can range from 60% to 90%, depending on factors such as the motor design, load, and operating conditions.

Common Features:

Permanent magnet or wound field construction

Brushed or brushless designs

Gearbox options for increased torque output

Encoders or Hall-effect sensors for speed and position feedback

Thermal protection to prevent overheating

5-1-3- lvdt

Fig 5.3 LVDT sensor

LVDT is an electromechanical device used to convert mechanical motion or vibrations, specifically rectilinear motion, into a variable electrical current, voltage or electric signals, and the reverse. Actuating mechanisms used primarily for automatic control systems or as mechanical motion sensors in measurement technologies. The classification of electromechanical transducers includes conversion principles or types of output signals.

LVDT SENSOR WITH ARDUINO

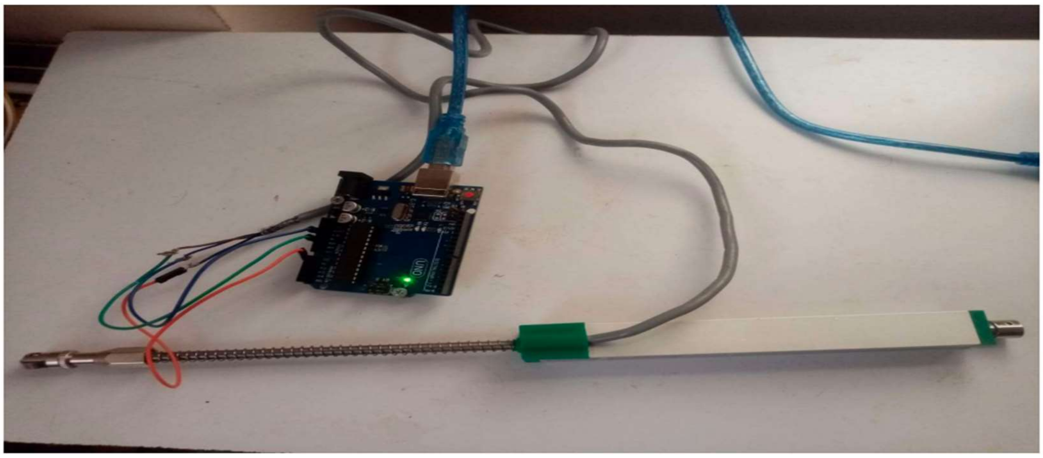

5-1-4-arduino Uno

The microcontroller used in the project is an Arduino Uno.

fig 5.4 Arduino uno

The Arduino Uno is an open-source microcontroller board based on the Microchip ATmega328P microcontroller developed by Arduino. cc and was initially released in 2010. The board is equipped with sets of digital and analog input/output (I/O) pins that may be interfaced with various expansion boards (shields) and other circuits. The board has 14 digital I/O pins (six capable of PWM output), and 6 analog I/O pins, and is programmable with the Arduino IDE (Integrated Development Environment), via a type B USB cable It can be powered by the USB cable or by an external 9-volt battery, though it accepts voltages between 7 and 20 volts.

Arduino Uno Specification

Microcontroller	ATmega328P
Operating Voltage	5V
Input Voltage (recommended)	7-12V
Input Voltage (limit)	6-20V
Digital I/O Pins	14 (of which 6 provide PWM output)
PWM Digital I/O Pins	6
Analog Input Pins	6
DC Current per I/O Pin	20 mA
DC Current for 3.3V Pin	50 mA
SRAM	2 KB (ATmega328P)
EEPROM	1 KB (ATmega328P)
Clock Speed	16 MHz
LED_BUILTIN	13
Length	68.6 mm
Width	53.4 mm
Weight	25 g

Table 5.1- Arduino Uno Specification

5-1-5- 6- PWM DC Motor Speed Controller
1-Input Voltage Range: 12-40 VDC
2-Maximum Current: 10A

A PWM DC Motor Speed Controller is a device used to control the speed of a DC motor by varying the duty cycle of

Power supplied to the motor. It works on the principle of PWM, where the motor is supplied with a series of

high frequency pulses, and the speed of the motor is controlled by varying the width (or duration) of these pulses.

3-Key Features and Functionality:

Input Voltage Range: The controller can operate with an input voltage ranging from 12 VDC to 40 VDC, which makes

It is suitable for a wide range of DC motor applications.

Maximum Current: The controller can handle a maximum current of 10A, which is sufficient for controlling

medium- sized DC motors.

PWM Control: The controller uses PWM technology to regulate the speed of the DC motor. By adjusting

the duty cycle of the PWM signal, the average voltage supplied to the motor is varied, resulting in speed control.

Overcurrent Protection: The controller typically includes overcurrent protection to prevent damage to the motor
and the controller itself in case of overload or short-circuit conditions.
Reverse Polarity Protection: The controller may have reverse polarity protection to prevent damage in case

the input power supply is connected with the wrong polarity.

Heat Sink: The controller may have a built-in heat sink to dissipate the heat generated during operation,

especially when the motor is under heavy load.

Control Input: The controller can be controlled using various input signals, such as a potentiometer, analog voltage,

or digital control signals (e.g., microcontroller, Arduino, Raspberry Pi).

4 LEVER LIMIT SWITCH

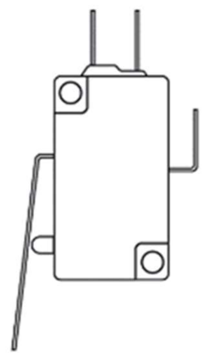

A limit switch is an electromechanical device operated by a physical force applied to it by an object.

Limit switches are used to detect the presence or absence of an object.

These switches were originally used to define the limit of travel of an object, and as a result, they were named Limit Switch.

Limit switch components

1. Actuator
2. Terminals
3. Built-in- switch (Head)

Electrical Specification:

Input Current:	0~5A
Output Current:	0.5-3.0A
Control Signal	: 3.3~24V
Power (MAX):	160W
Micro Step:	1, 2/A, 2/B, 4, 8, 16, 32
Temperature:	-10～45℃
Humidity:	No Condensation
Dimension:	96*56*33 mm
Weight:	0.2 kg
Drive IC:	TB67S109AFTG

Table 5.2- Electrical Specification of TB 6560 DRIVER

5-2 _Block diagram and code:

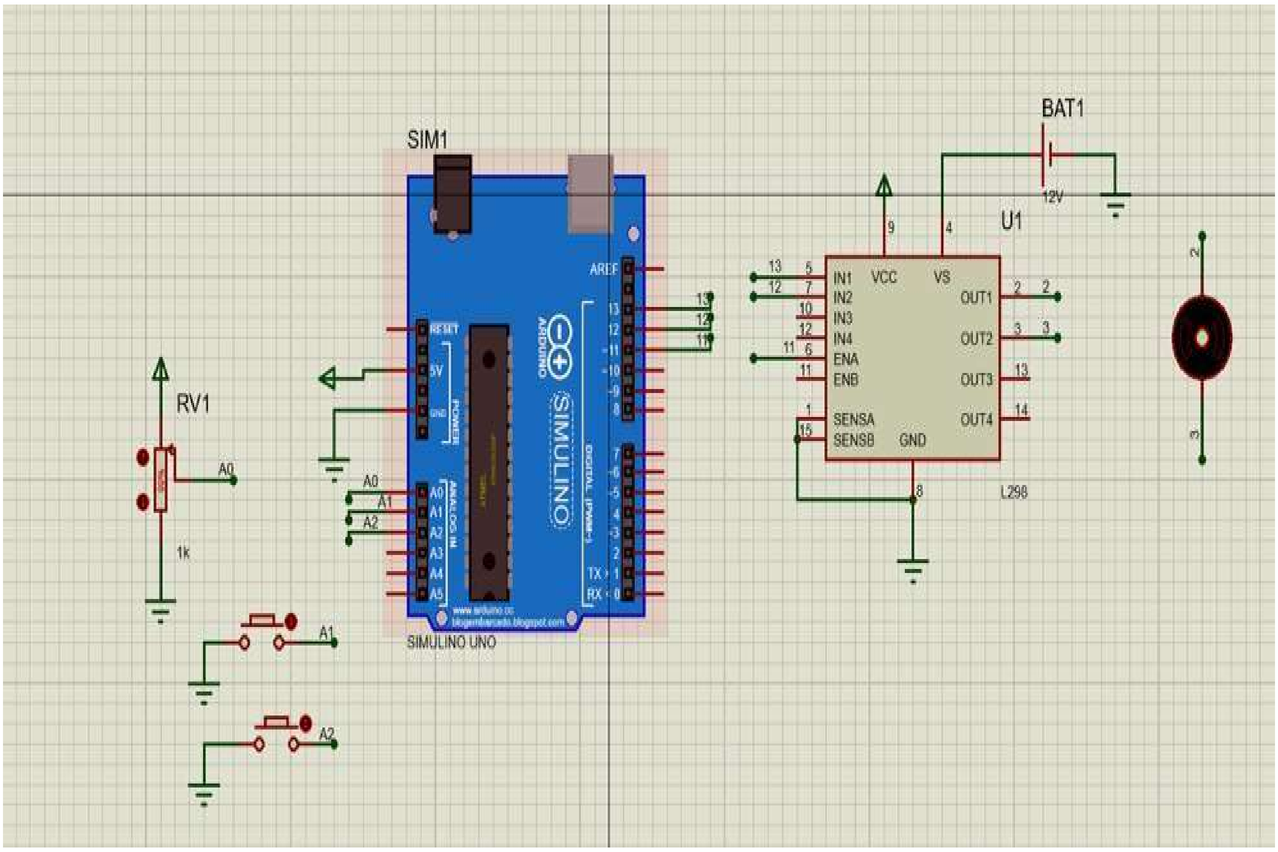

Fig 5.6 motor block diagram

Code:

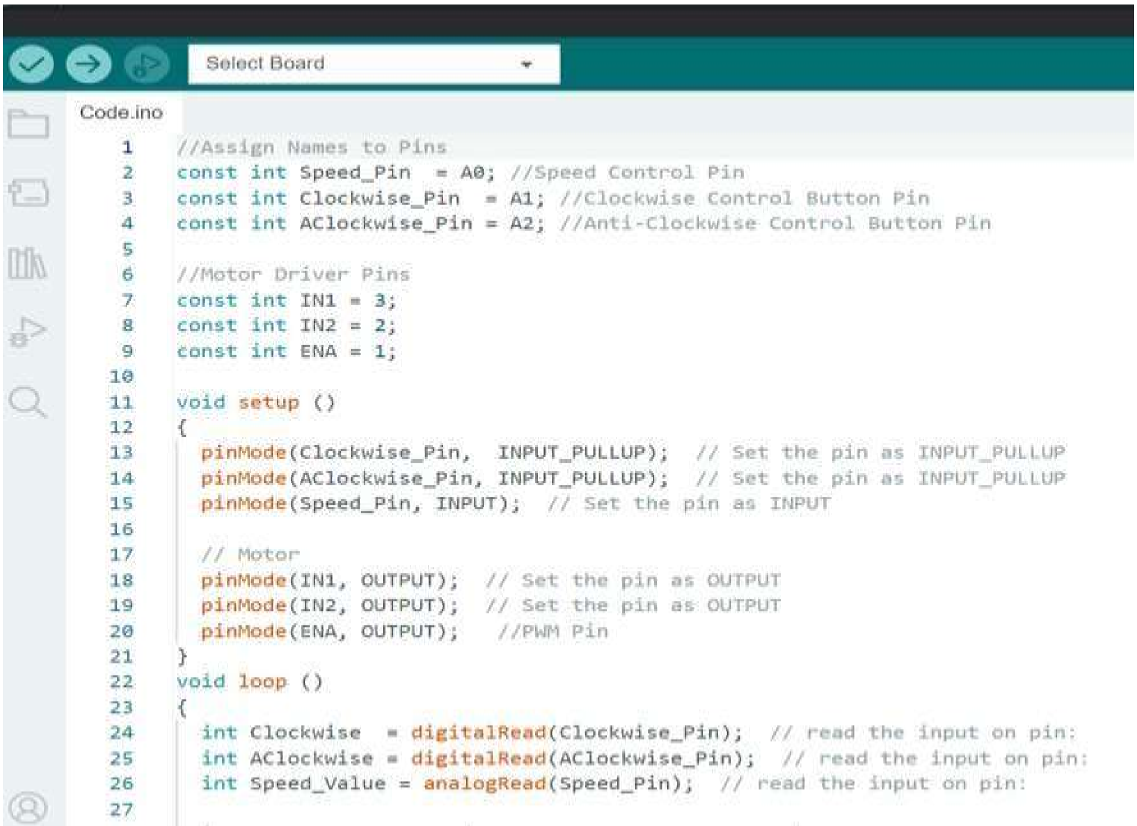


```
//Assign Names to Pins
const int Speed_Pin  = A0; //Speed Control Pin
const int Clockwise_Pin  = A1; //Clockwise Control Button Pin
const int AClockwise_Pin = A2; //Anti-Clockwise Control Button Pin

//Motor Driver Pins
const int IN1 = 3;
const int IN2 = 2;
const int ENA = 1;

void setup ()
{
  pinMode(Clockwise_Pin,  INPUT_PULLUP);  // Set the pin as INPUT_PULLUP
  pinMode(AClockwise_Pin, INPUT_PULLUP);  // Set the pin as INPUT_PULLUP
  pinMode(Speed_Pin, INPUT);  // Set the pin as INPUT

  // Motor
  pinMode(IN1, OUTPUT);  // Set the pin as OUTPUT
  pinMode(IN2, OUTPUT);  // Set the pin as OUTPUT
  pinMode(ENA, OUTPUT);   //PWM Pin
}
void loop ()
{
  int Clockwise  = digitalRead(Clockwise_Pin);  // read the input on pin:
  int AClockwise = digitalRead(AClockwise_Pin);  // read the input on pin:
  int Speed_Value = analogRead(Speed_Pin);  // read the input on pin:

```


```
int AClockwise = digitalRead(AClockwise_Pin);  // read the input on pin:
int Speed_Value = analogRead(Speed_Pin);  // read the input on pin:

int Motor_Speed = map(Speed_Value, 0,1023, 0,255);
analogWrite(ENA, Motor_Speed); //PWM Signal to control the speed of motor. (0 - 255)

if(Clockwise == LOW)
{
  // Start Motor Clockwise
  digitalWrite(IN1, HIGH);
  digitalWrite(IN2, LOW);
}

else if(AClockwise == LOW)
{
  // Start Motor Clockwise
  digitalWrite(IN1, LOW);
  digitalWrite(IN2, HIGH);
}

else
{
  // Start Motor Clockwise
  digitalWrite(IN1, LOW);
  digitalWrite(IN2, LOW);
}
}
```

Fig 5.7 arduino code

Code explains:

1-The code assigns names to the pin numbers for better readability.

2-setup() function is used to configure the pin modes. Clockwise Pin and A Clockwise Pin are set as INPUT_PULLUP, which means they are normally HIGH and pulled LOW when the corresponding buttons are pressed. Speed Pin is set as INPUT to read the speed control value.

3-The motor driver pins (IN1, IN2, and ENA) are set as OUTPUT.

4-In the loop() function, the code reads the state of the Clockwise Pin,

A Clockwise Pin, and the analog value from the Speed Pin.

5-The analog value from Speed Pin is mapped from the range 0-1023 to 0-255 to get the motor speed value.

6-The motor speed is controlled using analog Write() to the ENA pin with the calculated Motor Speed value.

7-If the Clockwise button is pressed (LOW), the motor is started in the clockwise direction by setting IN1 to HIGH and IN2 to LOW.

8-If the A Clockwise button is pressed (LOW), the motor is started in the anti-clockwise direction by setting IN1 to LOW and IN2 to HIGH.

9-If neither button is pressed, the motor is stopped by setting both IN1 and IN2 to LOW.

5-3 _Block diagram of lvdt:

Fig 5.8

LVDT block diagram

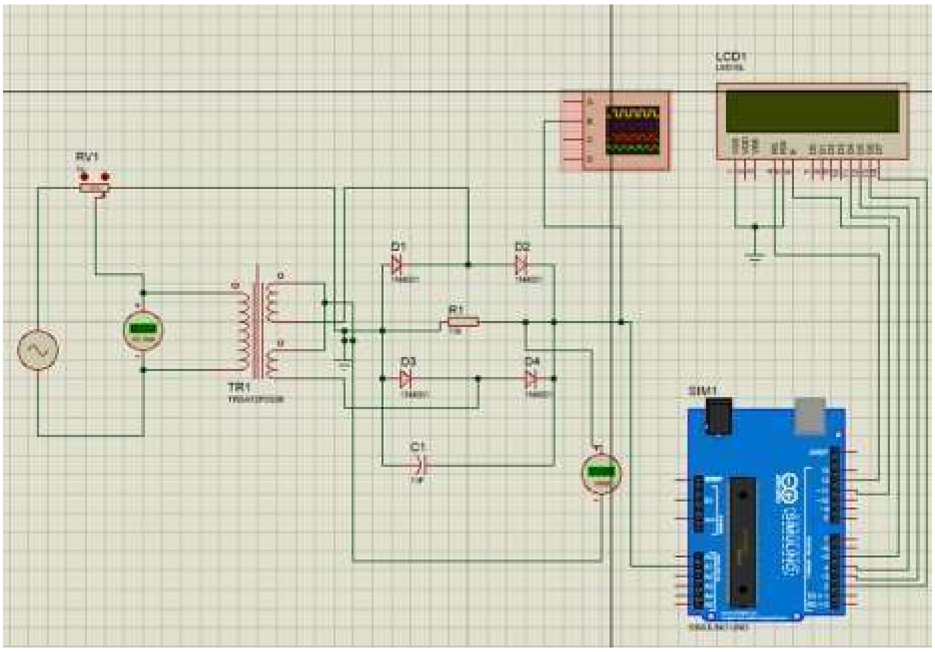

Code

```
#include <LiquidCrystal.h>
LiquidCrystal lcd(12, 11, 5, 4, 3, 2);

const int analogInPin = A1; // Analog pin 1 for reading the phototransistor
float Voltaje = 0;
float VoltaS = 0;

void setup() {
  Serial.begin(9600);

  lcd.begin(16, 2);
  lcd.clear();

  lcd.setCursor(0, 0);
  lcd.print("Sensor");

  lcd.setCursor(0, 1);
  lcd.print("LVTD");

  delay(500);
  lcd.clear();
}

void loop() {
  // Read the analog pin and assign the value to the variable.
  Voltaje = analogRead(analogInPin);

  VoltaS = Voltaje * (5.0 / 1023.0);

  lcd.setCursor(0, 0);
  lcd.print("Voltaje =");

  lcd.print(VoltaS, 2);
}
```

Fig 5.9

LVDT ARDUINO CODE

Code explains

1- The code includes the Liquid Crystal library to control the LCD display.

2- The Liquid Crystal object LCD is initialized with the appropriate pin numbers for RS, E, D4, D5, D6, and D7.

3- The analog input pin A1 is assigned to the variable amlodipine.

4- In the setup () function:

. Serial communication is initialized at a baud rate of 9600.

. The LCD is initialized with 16 columns and 2 rows using LCD. Begin (16, 2).

. The LCD is cleared, and the text "Sensor" is displayed on the first row and "LVTD" on the second row.

. There is a 500ms delay, and the LCD is cleared again.

5-In the loop () function:

. The analog value from anagliptin is read using analog Read () and assigned to the variable Voltage.

. The voltage is calculated by multiplying Voltage with the scaling factor of (5.0 / 1023.0) and assigned to Voltas.

. The LCD cursor is set to the first column of the first row using LCD. Set Cursor (0, 0).

. The text "Voltage =" is printed on the LCD.

. The calculated voltage value Voltas is printed on the LCD with two decimal places using LCD. Print (Voltas, 2).

6- The loop () function repeats continuously, reading the analog pin, calculating the voltage, and updating the LCD display with the new voltage value

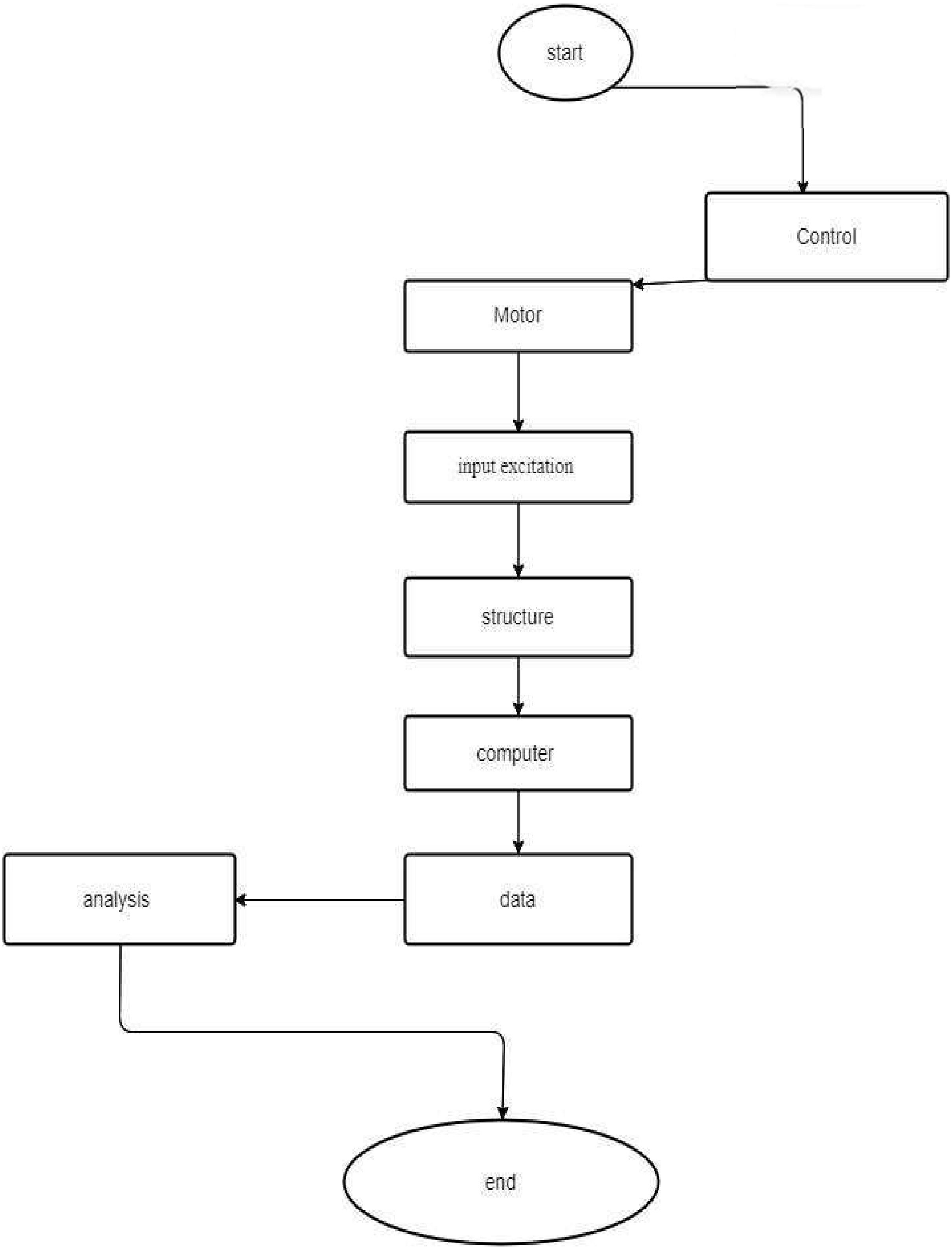
start
Control
Motor
input excitation
structure
computer
data
analysis
end

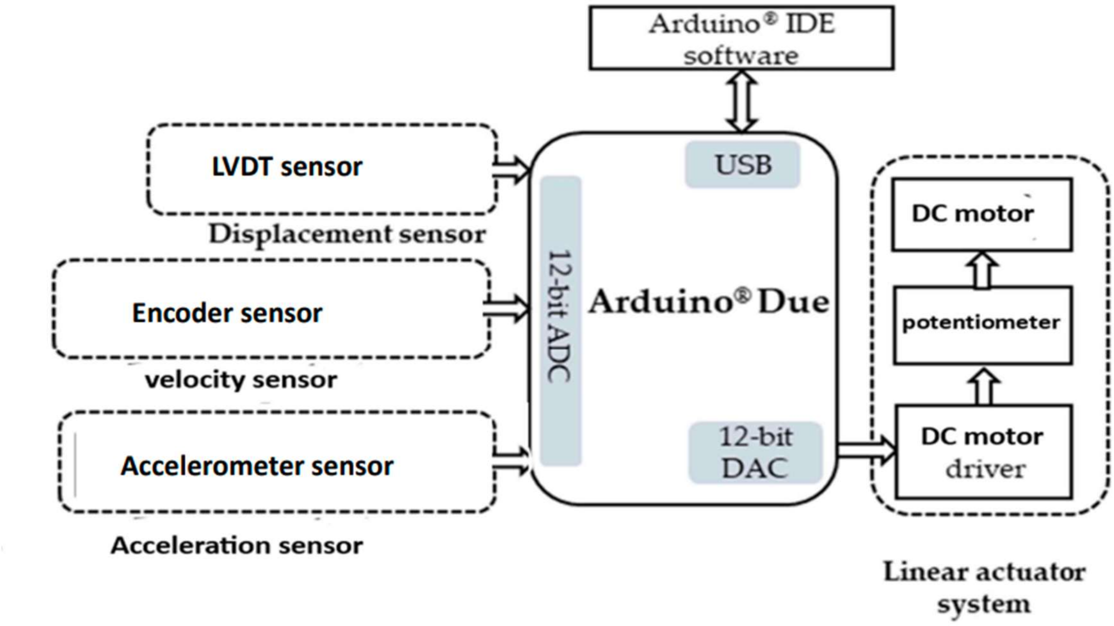

Block diagram of the data acquisition process.

Chapter 6
Appendices

6.1 Drawing sheets

Name part: Table

Material:` Balsa

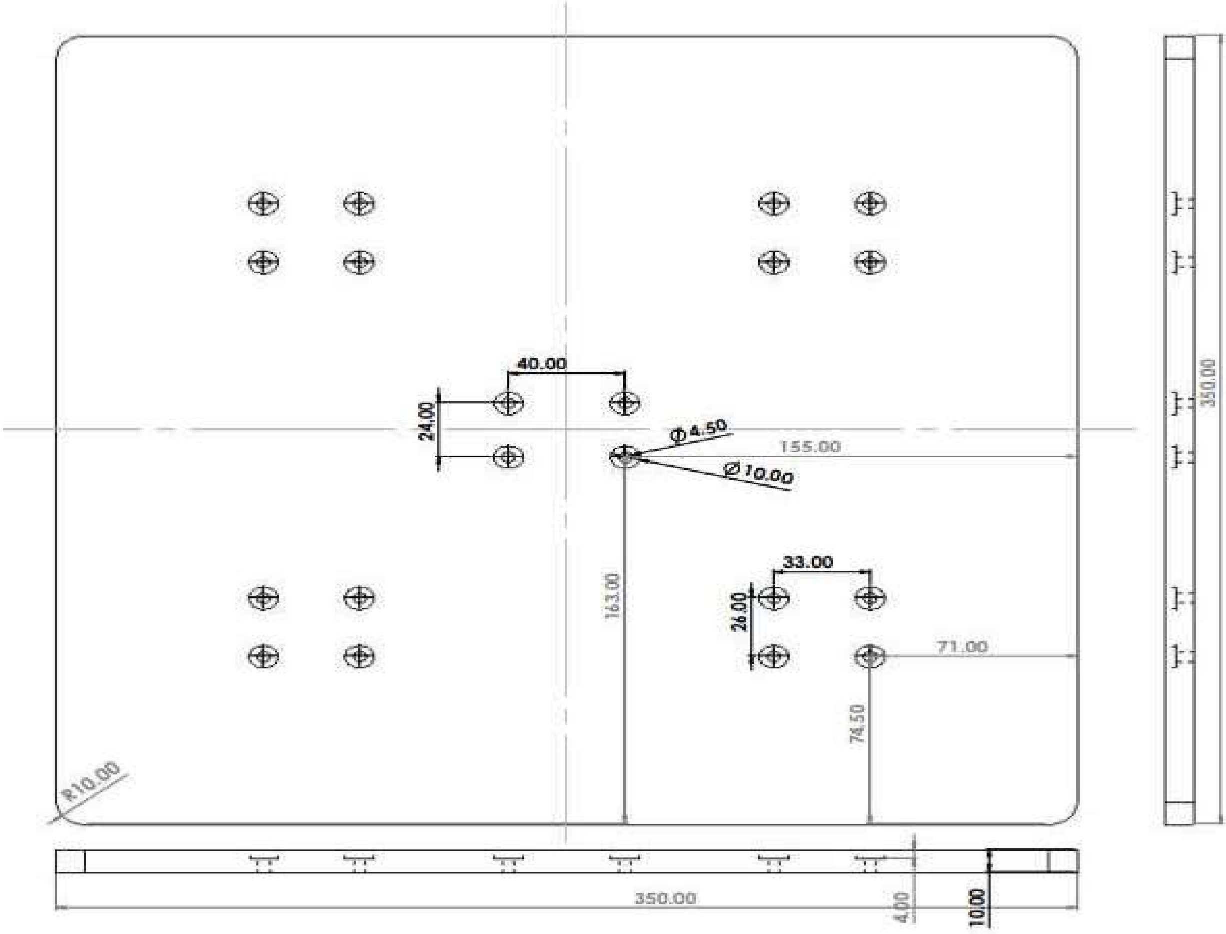

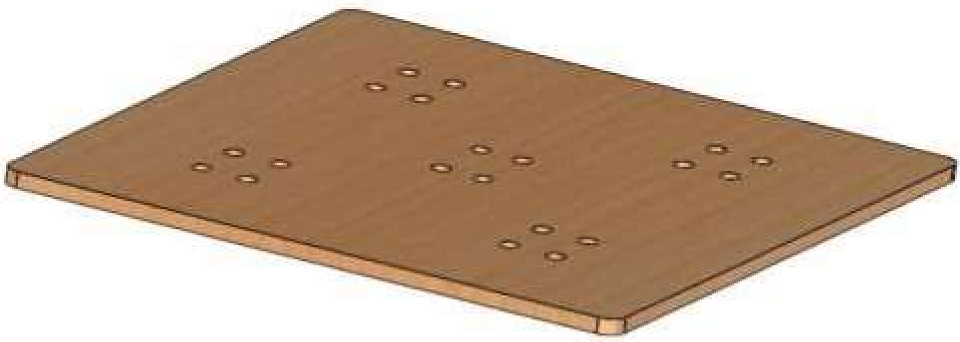

Fig 6.1 Tabe

Name part: Base Plate

Material: Balsa

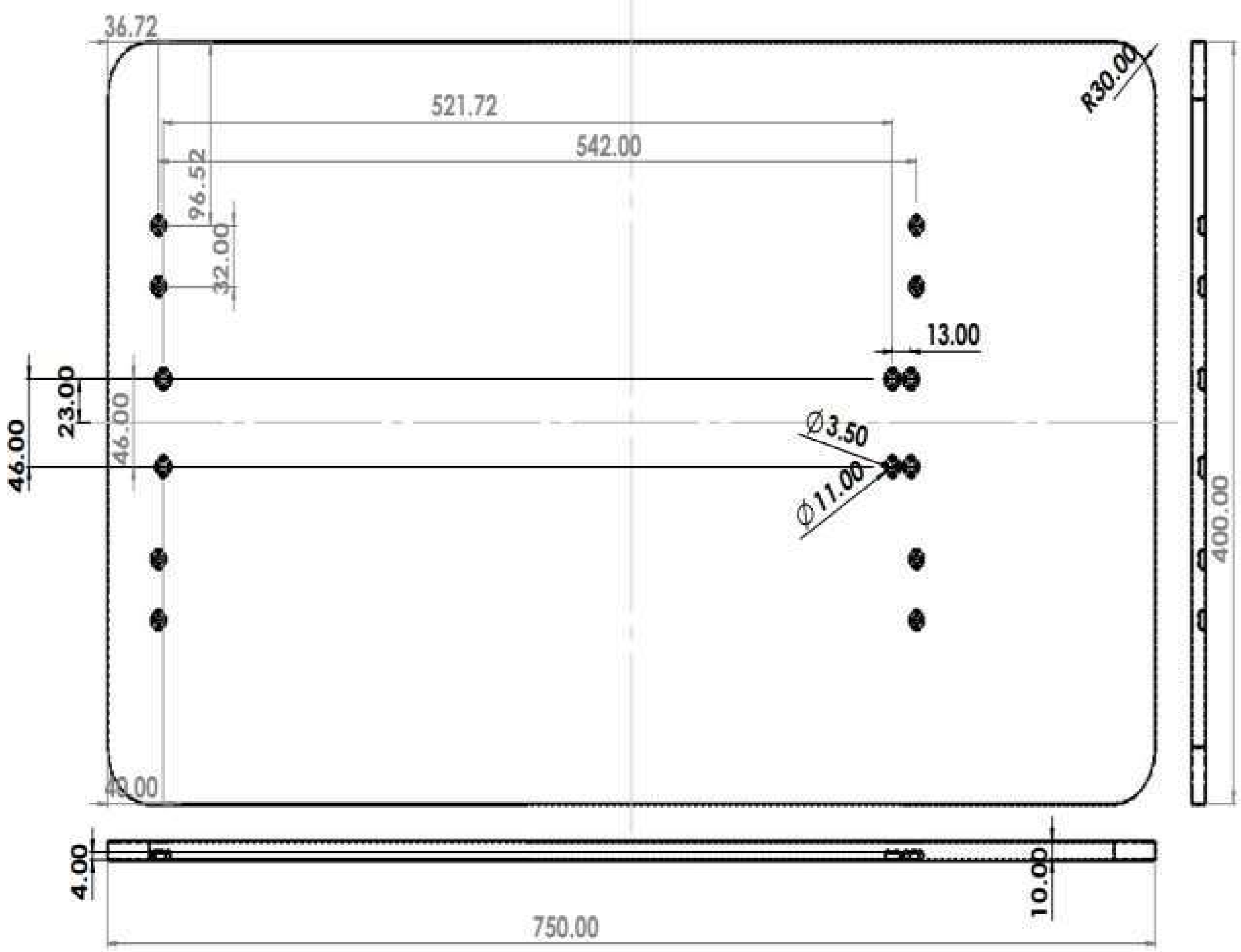

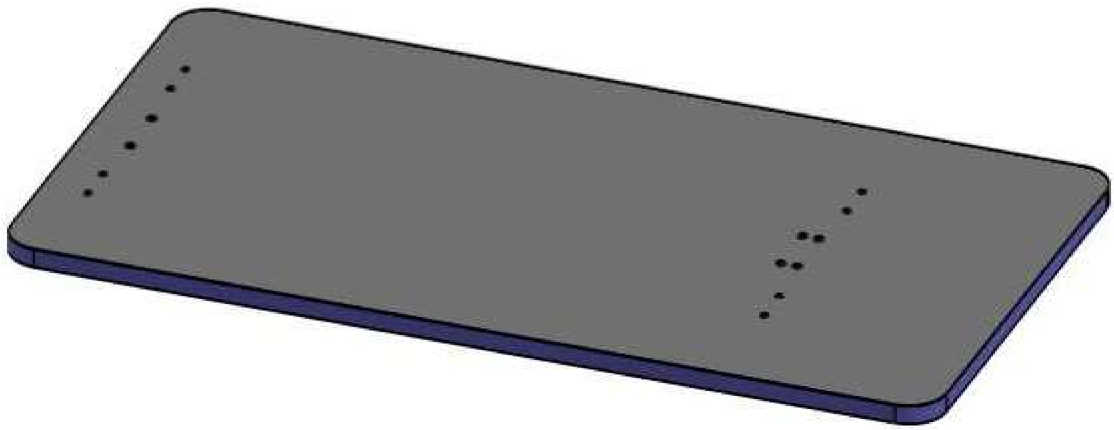

Fig 6.2-base plate

Name part: Lead nut

Material: Carbon Steel

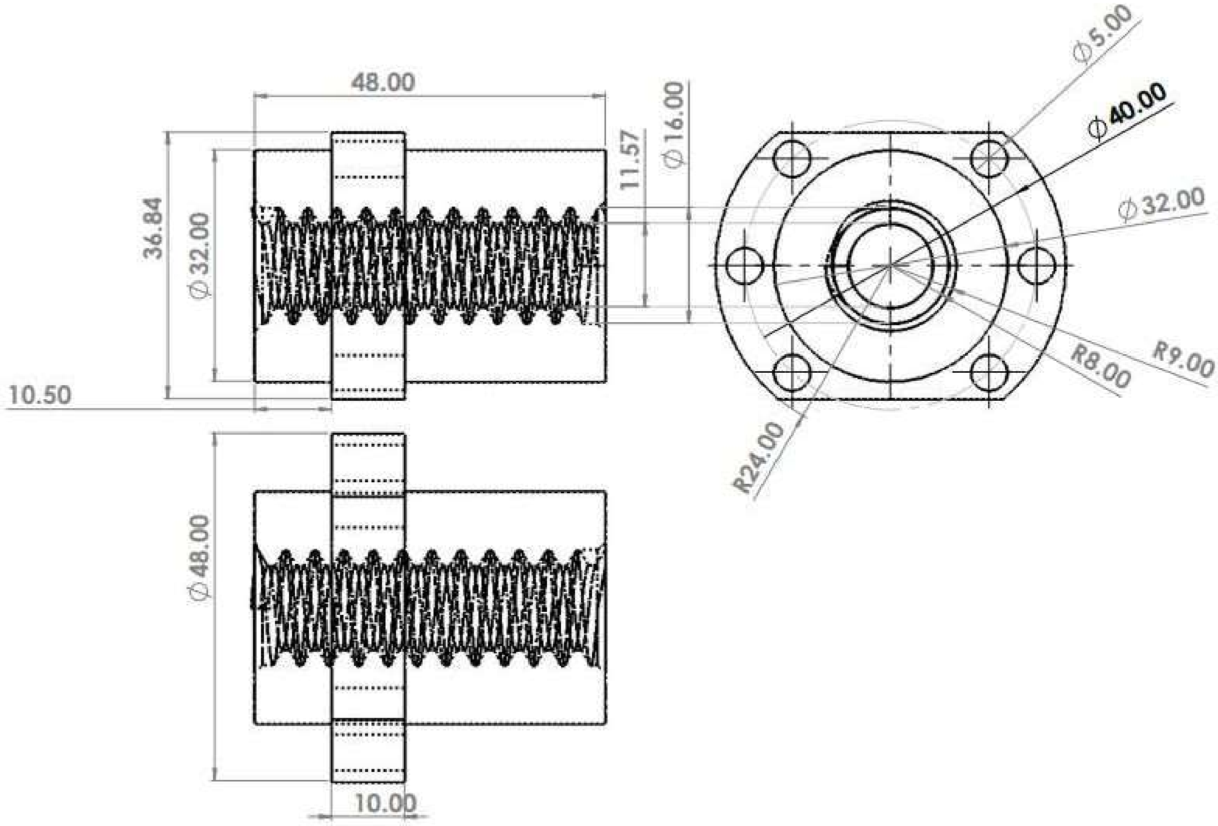

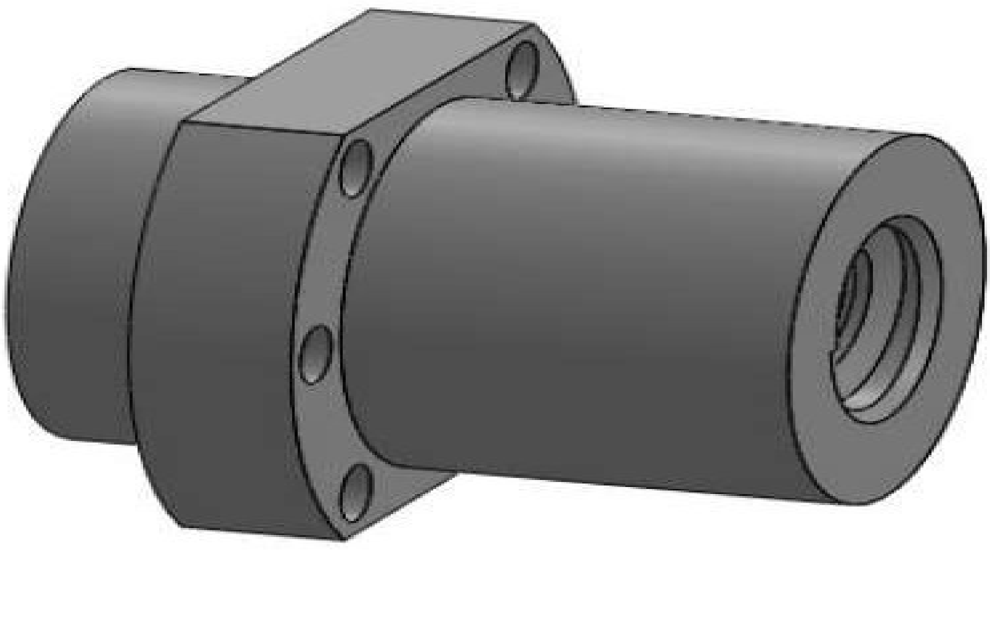

Fig 6.3 -lead nut

Name part: lead Screw Nut Seat Bracket Holder Mount Housing

Material: aluminum alloy

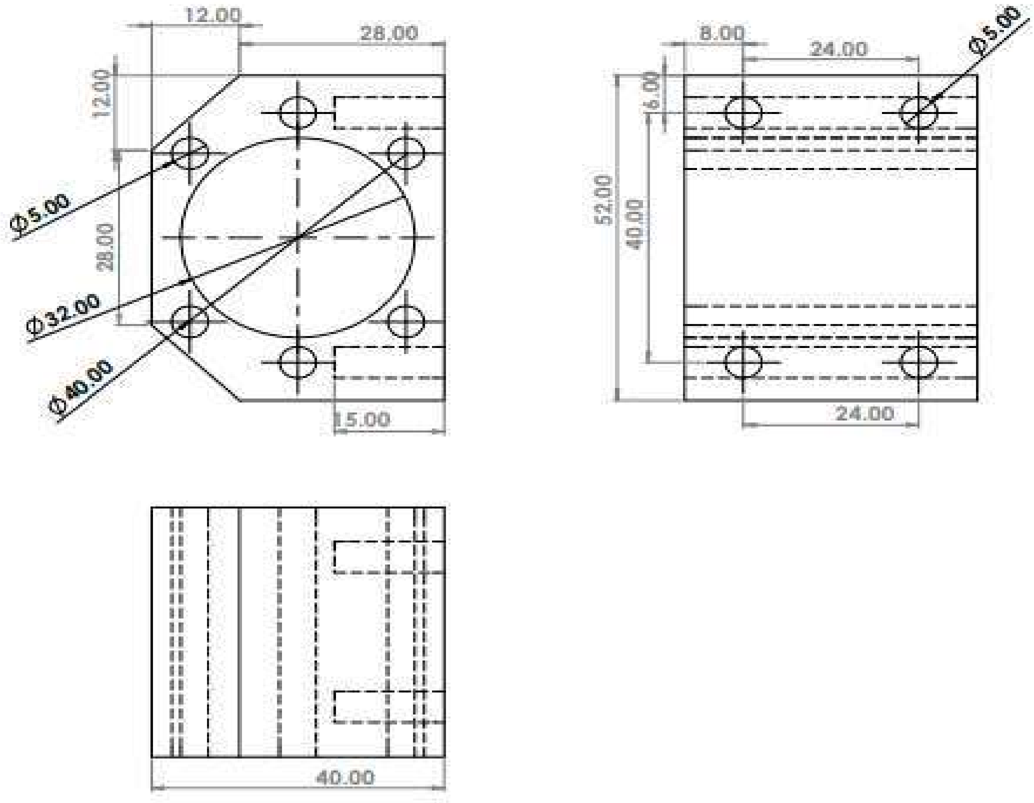

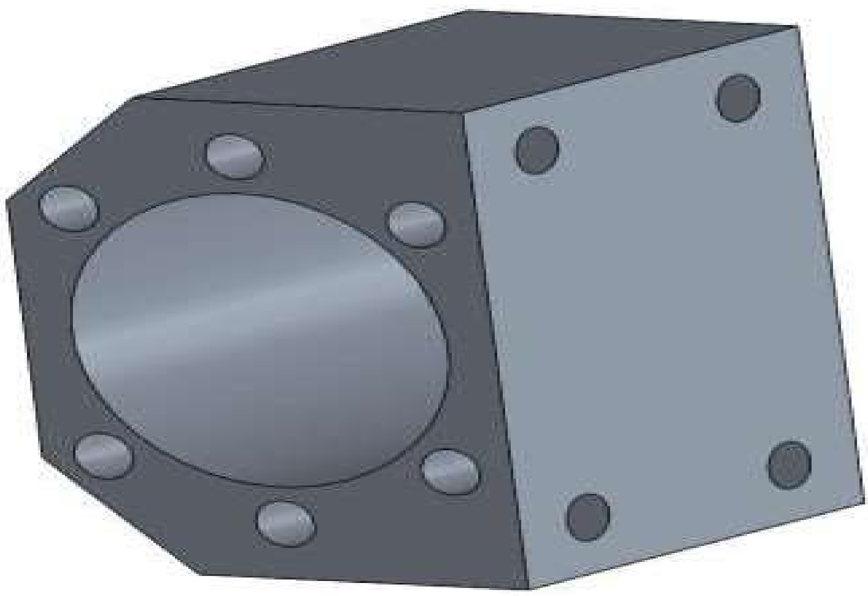

Fig 6.4- lead screw nut seat bracket holder mount housing

Name part: Linear Rail Shaft Support

Material: Carbon Steel

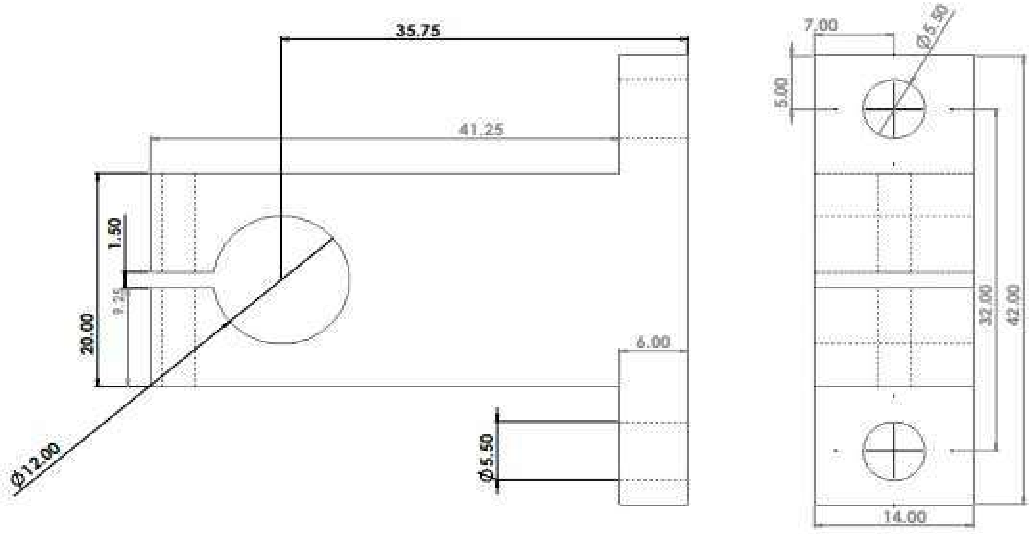

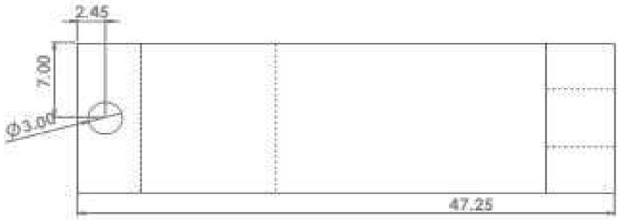

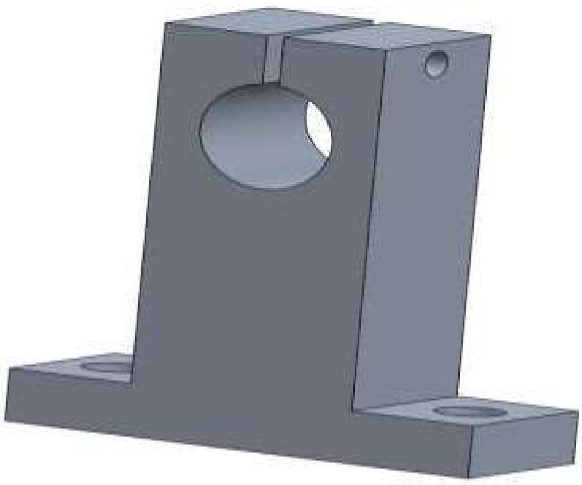

Fig 6.5- linear rail shaft support

Name part: Lead Screw End Supports

Material : Carbon Steel

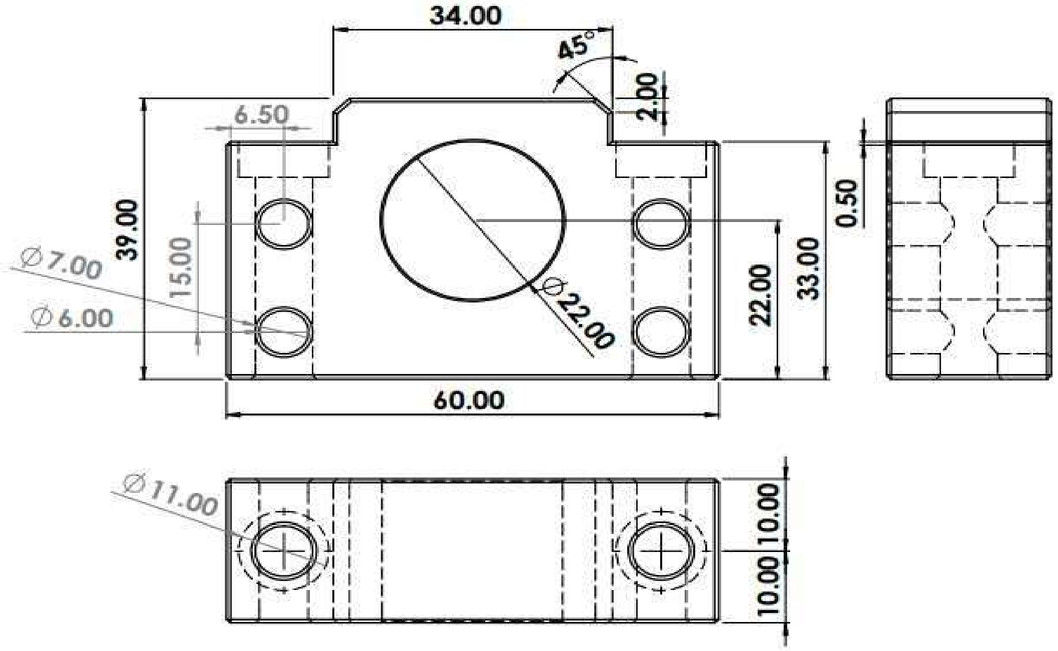

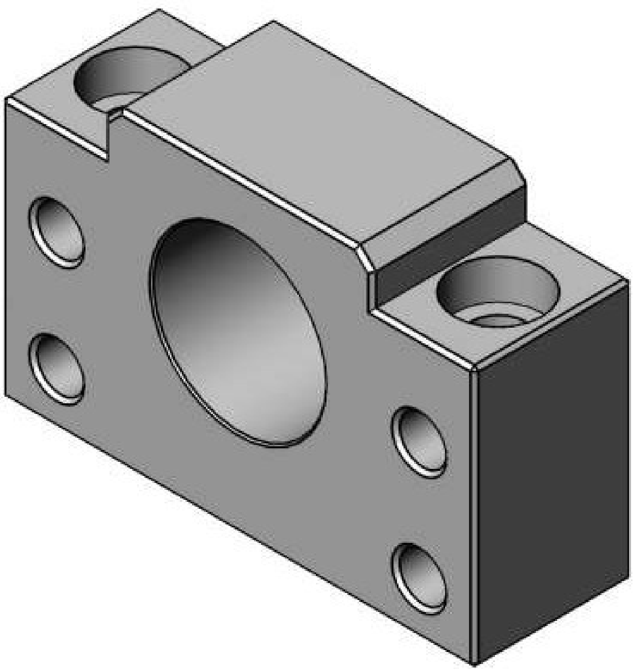

Fig 6.6-lead screw end supports

Name part: Lead Screw End Supports

Material: Carbon Steel

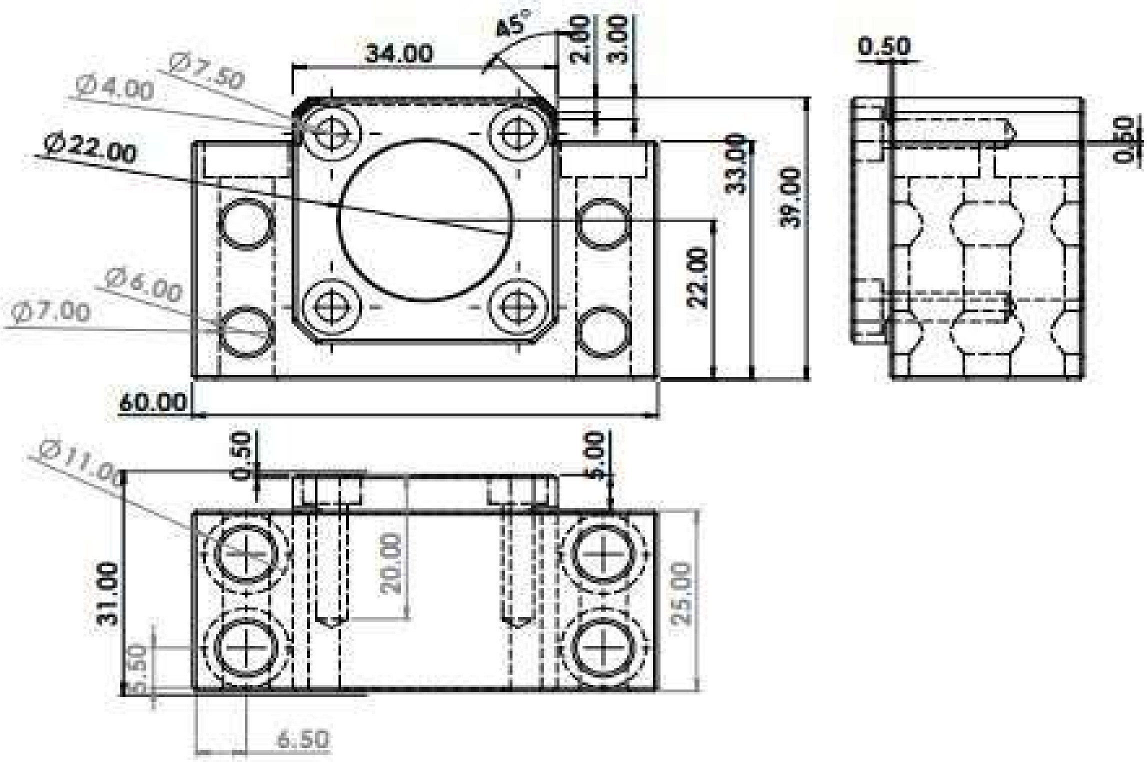

Fig 6.7-lead screw end supports.

Name part: Linear Motion Ball Slide Bearings
Material: Carbon Steel

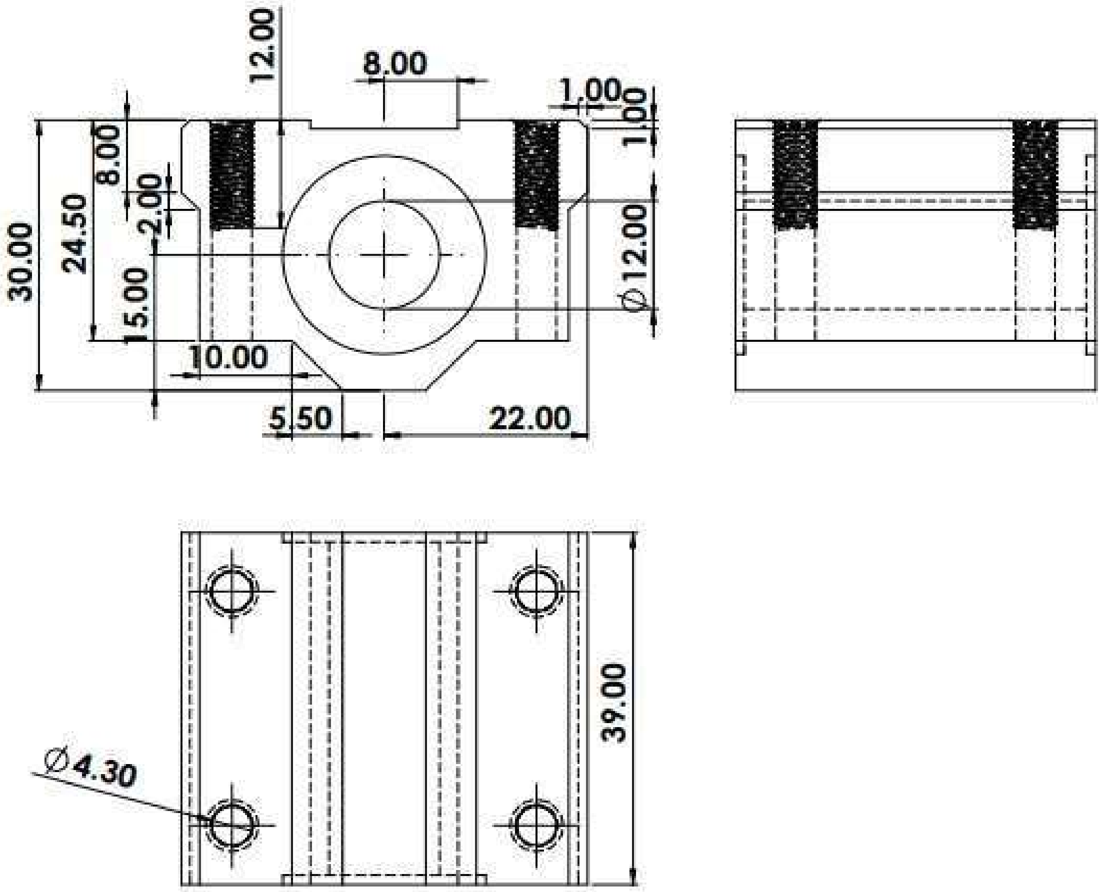

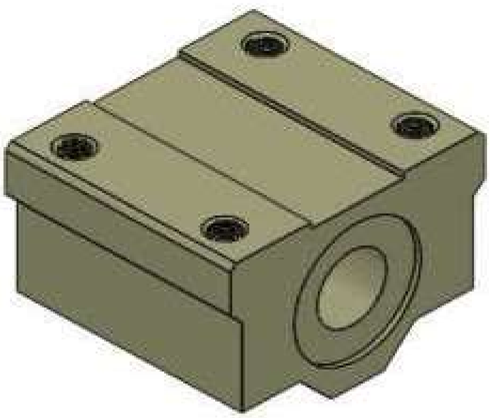

Fig 6.8-Linear Motion Ball Slide Bearings

Roller bearing

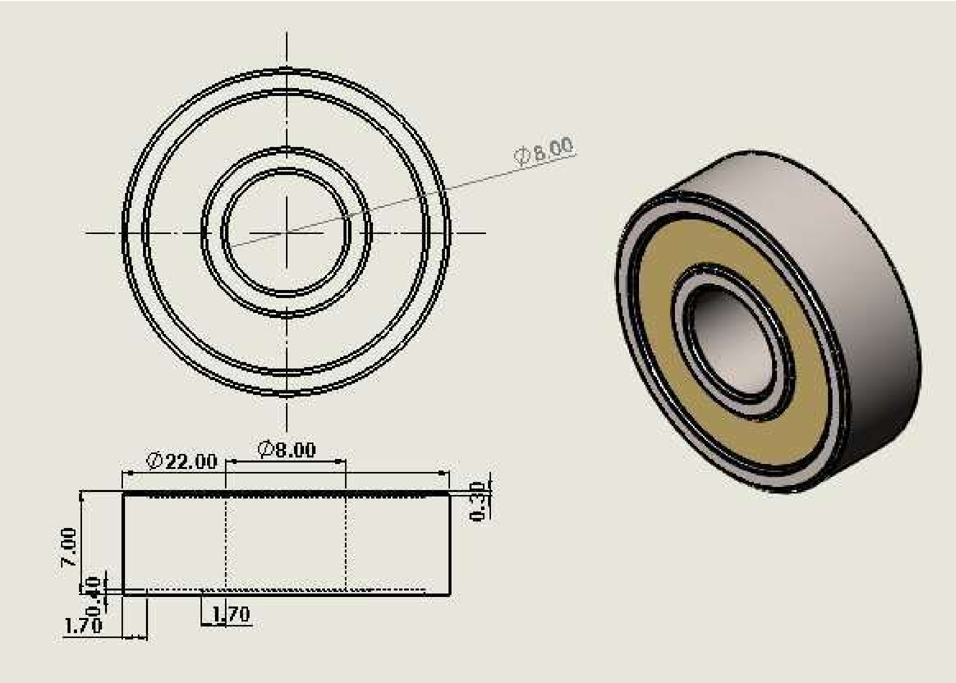

Fig 6.9-roller bearing.

Mass properties of Table

Configuration: Default
Coordinate system: -- default --

Density = 0.00 grams per cubic millimeter

Mass = 680.93 grams

Volume = 1215949.89 cubic millimeters

Surface area = 262230.20 square millimeters

Center of mass: (millimeters)
X = 0.00
Y = 5.01
Z = 0.00

Principal axes of inertia and principal moments of inertia: (grams * square millimeters)
Taken at the center of mass.

Ix = (0.00, 0.00, 1.00)	Px = 6964748.42
Iy = (1.00, 0.00, 0.00)	Py = 6965362.21
Iz = (0.00, 1.00, 0.00)	Pz = 13918773.20

Moments of inertia: (grams * square millimeters)
Taken at the center of mass and aligned with the output coordinate system.

Lxx = 6965362.21	Lxy = 0.00	Lxz = 0.00
Lyx = 0.00	Lyy = 13918773.20	Lyz = 0.00
Lzx = 0.00	Lzy = 0.00	Lzz = 6964748.42

Moments of inertia: (grams * square millimeters)
Taken at the output coordinate system.

Ixx = 6982469.79	Ixy = 0.00	Ixz = 0.00
Iyx = 0.00	Iyy = 13918773.20	Iyz = 0.00
Izx = 0.00	Izy = 0.00	Izz = 6981856.01

Mass properties of Base plate

Configuration: Default
Coordinate system: -- default --

Density = 0.01 grams per cubic millimeter

Mass = 24052.47 grams

Volume = 3006558.99 cubic millimeters

Surface area = 627595.66 square millimeters

Center of mass: (millimeters)
X = -0.28
Y = 5.07
Z = 0.00

Principal axes of inertia and principal moments of inertia: (grams * square millimeters)
Taken at the center of mass.

Ix = (1.00, 0.00, 0.00)	Px = 317704834.97
Iy = (0.00, 0.00, -1.00)	Py = 1125039099.40
Iz = (0.00, 1.00, 0.00)	Pz = 1442313703.00

Moments of inertia: (grams * square millimeters)
Taken at the center of mass and aligned with the output coordinate system.

Lxx = 317704840.48	Lxy = -78715.67	Lxz = 39.17
Lyx = -78715.67	Lyy = 1442313697.49	Lyz = 0.88
Lzx = 39.17	Lzy = 0.88	Lzz = 1125039099.40

Moments of inertia: (grams * square millimeters)
Taken at the output coordinate system.

Ixx = 318323221.58	Ixy = -112895.75	Ixz = 39.33
Iyx = -112895.75	Iyy = 1442315586.74	Iyz = -2.08
Izx = 39.33	Izy = -2.08	Izz = 1125659369.76

Mass properties of Lead screw

Configuration: Default

Coordinate system: -- default –

Density = 0.01 grams per cubic millimeter

Mass = 577.95 grams

Volume = 75058.89 cubic millimeters

Surface area = 42211.83 square millimeters

Center of mass: (millimeters)

X = 279.96

Y = 0.00

Z = 0.01

Principal axes of inertia and principal moments of inertia: (grams * square millimeters)

Taken at the center of mass.

Ix = (1.00, 0.00, 0.00)	Px = 13340.45
Iy = (0.00, 0.71, -0.70)	Py = 14576886.64
Iz = (0.00, 0.70, 0.71)	Pz = 14577623.13

Moments of inertia: (grams * square millimeters)

Taken at the center of mass and aligned with the output coordinate system.

Lxx = 13340.46	Lxy = -247.46	Lxz = 101.43
Lyx = -247.46	Lyy = 14577250.65	Lyz = -368.23
Lzx = 101.43	Lzy = -368.23	Lzz = 14577259.11

Moments of inertia: (grams * square millimeters)

Taken at the output coordinate system.

Ixx = 13340.49	Ixy = -870.78	Ixz = 1032.93
Iyx = -870.78	Iyy = 59874729.99	Iyz = -368.24
Izx = 1032.93	Izy = -368.24	Izz = 59874738.44

Mass properties of guide shafts

Configuration: Default
Coordinate system: -- default --

Density = 0.01 grams per cubic millimeter

Mass = 483.92 grams

Volume = 62846.51 cubic millimeters

Surface area = 21140.13 square millimeters

Center of mass: (millimeters)
X = 278.00
Y = 0.00
Z = 0.00

Principal axes of inertia and principal moments of inertia: (grams * square millimeters)
Taken at the center of mass.

Ix = (1.00, 0.00, 0.00)	Px = 8706.61
Iy = (0.00, 0.00, -1.00)	Py = 12456656.68
Iz = (0.00, 1.00, 0.00)	Pz = 12456656.68

Moments of inertia: (grams * square millimeters)
Taken at the center of mass and aligned with the output coordinate system.

Lxx = 8706.61	Lxy = 0.00	Lxz = 0.00
Lyx = 0.00	Lyy = 12456656.68	Lyz = 0.00
Lzx = 0.00	Lzy = 0.00	Lzz = 12456656.68

Moments of inertia: (grams * square millimeters)
Taken at the output coordinate system.

Ixx = 8706.61	Ixy = 0.00	Ixz = 0.
Iyx = 0.00	Iyy = 49855788.06	Iyz = 0.00
Izx = 0.00	Izy = 0.00	Izz = 49855788.06

Mass properties of Lead Screw End Supports

Configuration: Default
Coordinate system: -- default --

Density = 0.00 grams per cubic millimeter

Mass = 48.57 grams

Volume = 48570.57 cubic millimeter

Surface area = 23080.31 square millimeters

Center of mass: (millimeters)
X = 0.00
Y = -3.55
Z = 1.31

Principal axes of inertia and principal moments of inertia: (grams * square millimeters)
Taken at the center of mass.

Ix = (1.00, 0.00, 0.00)	Px = 9014.86
Iy = (0.00, 1.00, 0.09)	Py = 14725.51
Iz = (0.00, -0.09, 1.00)	Pz = 17272.42

Moments of inertia: (grams * square millimeters)
Taken at the center of mass and aligned with the output coordinate system.

Lxx = 9014.86	Lxy = 0.00	Lxz = 0.02
Lyx = 0.00	Lyy = 14745.64	Lyz = 225.55
Lzx = 0.02	Lzy = 225.55	Lzz = 17252.29

Moments of inertia: (grams * square millimeters)
Taken at the output coordinate system.

Ixx = 9709.89	Ixy = -0.01	Ixz = 0.02
Iyx = -0.01	Iyy = 14829.41	Iyz = -0.73
Izx = 0.02	Izy = -0.73	Izz = 17863.55

Mass properties of lead Screw Nut Seat Bracket Holder Mount Housing

Configuration: Default

Coordinate system: -- default --

Density = 0.00 grams per cubic millimeter

Mass = 106.32 grams

Volume = 39379.61 cubic millimeters

Surface area = 17559.16 square millimeters

Center of mass: (millimeters)

X = 21.97

Y = 20.00

Z = 26.00

Principal axes of inertia and principal moments of inertia: (grams * square millimeters)

Taken at the center of mass.

Ix = (0.00, 0.00, 1.00)	Px = 31589.90
Iy = (1.00, 0.00, 0.00)	Py = 47007.05
Iz = (0.00, 1.00, 0.00)	Pz = 50321.43

Moments of inertia: (grams * square millimeters)

Taken at the center of mass and aligned with the output coordinate system.

Lxx = 47007.05	Lxy = 0.00	Lxz = 0.00
Lyx = 0.00	Lyy = 50321.43	Lyz = 0.00
Lzx = 0.00	Lzy = 0.00	Lzz = 31589.90

Moments of inertia: (grams * square millimeters)

Taken at the output coordinate system.

Ixx = 161412.68	Ixy = 46711.40	Ixz = 60724.82
Iyx = 46711.40	Iyy = 173501.02	Iyz = 55288.97
Izx = 60724.82	Izy = 55288.97	Izz = 125423.80

Mass properties of Lead nut

Configuration: Varsayılan
Coordinate system: -- default --

Density = 0.01 grams per cubic millimeter

Mass = 297.73 grams

Volume = 37888.67 cubic millimeters

Surface area = 11995.48 square millimeters

Center of mass: (millimeters)
X = 22.52
Y = 0.01
Z = 0.01

Principal axes of inertia and principal moments of inertia: (grams * square millimeters)
Taken at the center of mass.

Ix = (1.00, 0.00, 0.00)	Px = 57677.23
Iy = (0.00, 0.00, -1.00)	Py = 76069.24
Iz = (0.00, 1.00, 0.00)	Pz = 82083.07

Moments of inertia: (grams * square millimeters)
Taken at the center of mass and aligned with the output coordinate system.

Lxx = 57677.40	Lxy = 41.79	Lxz = -41.78
Lyx = 41.79	Lyy = 82082.98	Lyz = 8.67
Lzx = -41.78	Lzy = 8.67	Lzz = 76069.16

Moments of inertia: (grams * square millimeters)
Taken at the output coordinate system.

Ixx = 57677.44	Ixy = 93.82	Ixz = 12.92
Iyx = 93.82	Iyy = 233043.06	Iyz = 8.69
Izx = 12.92	Izy = 8.69	Izz = 227029.24

Mass properties of Linear Motion Ball Slide Bearings

Configuration: Default
Coordinate system: -- default --

Density = 0.01 grams per cubic millimeter

Mass = 278.09 grams

Volume = 35653.18 cubic millimeters

Surface area = 10321.94 square millimeters

Center of mass: (millimeters)
X = 0.00
Y = 16.93
Z = 0.00

Principal axes of inertia and principal moments of inertia: (grams * square millimeters)
Taken at the center of mass.

Ix = (0.00, 0.00, 1.00)	Px = 52435.51
Iy = (1.00, 0.00, 0.00)	Py = 59850.90
Iz = (0.00, 1.00, 0.00)	Pz = 74961.31

Moments of inertia: (grams * square millimeters)
Taken at the center of mass and aligned with the output coordinate system.

Lxx = 59850.90	Lxy = 0.00	Lxz = -0.47
Lyx = 0.00	Lyy = 74961.31	Lyz = 0.00
Lzx = -0.47	Lzy = 0.00	Lzz = 52435.51

Moments of inertia: (grams * square millimeters)
Taken at the output coordinate system.

Ixx = 139553.54	Ixy = 0.00	Ixz = -0.47
Iyx = 0.00	Iyy = 74961.31	Iyz = 0.00
Izx = -0.47	Izy = 0.00	Izz = 132138.15

Mass properties of Linear Rail Shaft Support

Configuration: Valor predeterminado
Coordinate system: -- default --

Density = 0.00 grams per cubic millimeter

Mass = 34.93 grams
Volume = 12936.08 cubic millimeters

Surface area = 5313.30 square millimeters

Center of mass: (millimeters)
X = -19.23
Y = 21.00
Z = 7.00

Principal axes of inertia and principal moments of inertia: (grams * square millimeters)
Taken at the center of mass.

Ix = (1.00, 0.00, 0.00)	Px = 2775.58
Iy = (0.00, 1.00, 0.00)	Py = 7401.86
Iz = (0.00, 0.00, 1.00)	Pz = 9000.92

Moments of inertia: (grams * square millimeters)
Taken at the center of mass and aligned with the output coordinate system.

Lxx = 2775.58	Lxy = 0.00	Lxz = 0.00
Lyx = 0.00	Lyy = 7401.86	Lyz = 0.00
Lzx = 0.00	Lzy = 0.00	Lzz = 9000.92

Moments of inertia: (grams * square millimeters)
Taken at the output coordinate system.

Ixx = 19890.02	Ixy = -14101.88	Ixz = -4700.63
Iyx = -14101.88	Iyy = 22023.97	Iyz = 5134.33
Izx = -4700.63	Izy = 5134.33	Izz = 37314.58

Chapter 7
Conclusion

Conclusion

Our one-direction shake table test has unearthed significant insights into the earthquake resistance of the studied structure(s) or component(s). Simulated seismic loading unveiled crucial details about its behavior, including its strength, deformation patterns, failure modes, and dynamic characteristics. These observations have both validated and challenged our initial design assumptions, exposing potential vulnerabilities previously unaccounted for. The effectiveness of implemented mitigation strategies, like base isolation systems or energy dissipation devices, has been rigorously evaluated, guiding us towards recommendations for design improvements, construction practices, and avenues for future research. While acknowledging the inherent limitations of our testing, such as simplified loading conditions and inherent scale effects, we cannot overstate the importance of shake table testing in verifying and ultimately enhancing the earthquake resilience of our structures. This knowledge not only strengthens our specific project but also contributes valuable data to the ongoing quest for safer, more resilient infrastructure in the face of seismic threats.

Chapter 8

cost

Cost Of Shake Table

Id	Components	cost
1.	Accelerometer sensor	170,00 ج.م.
2.	LVDT sensor	مستخدم من قسم مدني
3.	Arduino nano shield	110,00 ج.م.
4.	Motor DC (24v)	470,00 ج.م.
5.	Lead screw/500mm	120ج.م
6.	linear guide(1 Meter)	120.ج.م
7.	Linear motion ball bearing	210.ج.م
8.	Nuts(one price)	20,00 ج.م.
9.	Washer(one price)	10,00 ج.م.
10.	Lead screw housing nut	75,00 ج.م.
11.	Arduino uno	680.ج.م
12.	Limit switch(2)	100,00 ج.م.
13.	Base plate	200,00 ج.م.
14.	plate	170.ج.م
15.	Pwm DC motor speed control	300,00 ج.م.
16.	Power supply(24v,15A)	100,00 ج.م.
17.	Usb موزع	90,00 ج.م.
18.	Relay module shield 4 channel	720,00 ج.م.
19.	Arduino usb cable(2)	60,00 ج.م.
20.	LCD2004 blue(2)	750,00 ج.م.
TOTAL		4205,00 ج.م.

Table 8.1: cost of shake table

Chapter 9
References

References

Introduction and Conclusion References

- https://www.usgs.gov/programs/earthquake-hazards/earthquakes
- https://www.ancoengineers.com/PUB%20SEISMICTESTINGINTRO.pdf
- For concrete structures: Pauley, T., & Priestley, M. J. N. (2017). Seismic design of reinforced concrete and masonry structures. John Wiley & Sons.

1. Controller development for the E-Defense shaking table.
2. Nakashima, M. Test on collapse behavior of structural systems. Sci. Technol. Japan, 2006, 96, 14–19.

3- Earthquake Induced Liquefaction Using Shak e Induced Liquefaction Using Shake Table Test
S. R. Pathak
College of Engineering, Pune, India
R. S. Dalvi
College of Engineering, Pune, India
A. D. Katdare
B. College of Engineering, Pune, India

4. SHAKING TABLE - STRUCTURE INTERACTION by ABDULKARIM M. RINAWI RAY W. CLOUGH

5-A textbook of machine design, R.S. KHURMI J.K. GUPTA , 2005

6- cost References

- https://www.juthour-tech.com/en/
- https://ram-e-shop.com/

Introduction and Conclusion References

- https://www.usgs.gov/programs/earthquake-hazards/earthquakes
- https://www.ancoengineers.com/PUB%20SEISMICTESTINGINTRO.pdf
- For concrete structures: Pauley, T., & Priestley, M. J. N. (2017). Seismic design of reinforced concrete and masonry structures. John Wiley & Sons.